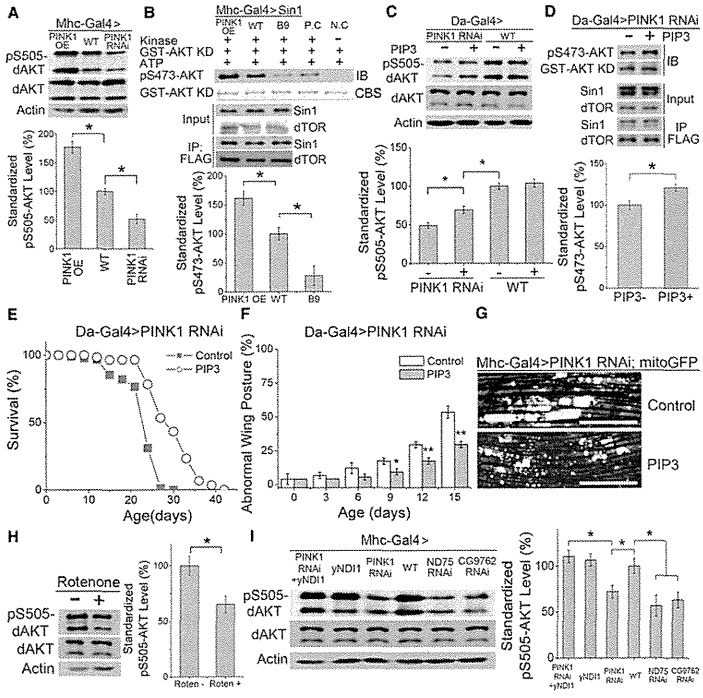

Figure 2. Effects of PINK1 and mitochondrial CI function on TORC2 activity. (*A*) Western blot analysis of *Mhc-Gal4*-driven control (wild type [WT]), PINK1 overexpression, and PINK1-RNAi muscle extracts with the indicated antibodies and data quantification. (*B, top*) In vitro phosphorylation of recombinant human GST-AKT-KD by *Drosophila* TORC2 affinity-purified from control, PINK1-overexpressing, and PINK1 LOF animals, all expressing a Sin1-Flag transgene. (*Bottom*) Similar amounts of Sin1 and dTOR were present in the extracts or immunoprecipitated TORC2. After kinase reaction, AKT phosphorylation was detected with anti-pS473-AKT, and total GST-AKT-KD was detected by Coomassie Blue staining (CBS). (P.C.) Positive control with extract added; (N.C.) negative control with no kinase added. Bar graph shows data quantification. (*C–G*) The rescuing effect of PIP3 treatment on in vivo p-S505-AKT level (*C*), in vitro mTORC2 kinase activity (*D*), lifespan (*E*), wing posture (*F*), and muscle mitochondrial morphology (*G*) in PINK1-RNAi animals. Values represent relative protein amounts after normalization with controls. Mitochondrial morphology was monitored with a mito-GFP reporter. In vitro mTORC2 kinase assay was performed as in *B*. Bar graphs show data quantification. Bar, 30 μm. (*H*) Reduction of pS505-AKT level by rotenone treatment of wild-type animals. (*I*) Effect of CI subunit (ND75 and CG9762) RNAi on pS505-AKT level and restoration of the p-S505-AKT level in PINK1-RNAi animals after yNDI1 coexpression. Values represent relative protein amounts after normalization with controls. Bar graphs show data quantification. (*) $P < 0.05$ in one-way ANOVA or Student's *t*-tests.

whereas the rescue of *dPINK1* LOF phenotypes by Rictor overexpression was fully blocked by Trc LOF transgenes (Supplemental Fig. S6B,D). Moreover, Trc RNAi induced mitochondrial aggregation and DN loss in a wild-type background (Supplemental Fig. S7A–C). These results thus establish Trc as a key component of the PINK1 pathway in MQC and tissue maintenance.

We further explored the biochemical mechanism of the signaling events involving PINK1, mTORC2, and Trc. Consistent with Trc acting downstream from PINK1, phosphorylation of Trc at S292 and T453, which correlate with Trc activation (Emoto et al. 2006), were reduced in *dPINK1* mutants but significantly increased in PINK1 GOF flies (Fig. 3F). This was further supported by in vitro assays of kinase activities of Trc purified from PINK1 LOF and GOF flies using phosphorylation of AAK1, a newly identified substrate of mammalian NDR (Ultanir et al. 2012), as readout (Fig. 3G). Interestingly, the effect of PINK1 on T453 site phosphorylation was mTORC2-dependent, whereas its effect on S292 was mTORC2-independent (Fig. 3H), suggesting that PINK1 regulates these two phosphorylation events through distinct mechanisms. We next tested whether activated Trc is localized to mitochondria to exert its effects on MQC. Strikingly, p-T453-Trc and p-S292-Trc were found primarily in the mitochondrial fraction, whereas total Trc was found in both the cytoplasmic and mitochondrial fractions (Supplemental Fig. S8A). Since mTORC2 is also localized to mitochondria (Supplemental Fig. S8B), mitochondria may serve as a novel platform for mTORC2 and Trc signaling.

Parkin plays a critical role in MQC and maintenance of muscle and DNs and acts downstream from PINK1. We found that the LOF effects of Rictor (Fig. 4A,E) or Trc (Fig. 4C,G) in enhancing *dPINK1* mutant phenotypes were completely blocked by Parkin GOF, suggesting that Parkin acts downstream from TORC2 and Trc in the PINK1 pathway. Consistently, Rictor GOF (Fig. 4B,F) or Trc GOF (Fig. 4D,H) failed to rescue the abnormal wing posture and mitochondrial morphology phenotypes of the *parkin* mutant. Next, we tested the genetic interaction between mTORC2/Trc and key executors of MQC known to genetically interact with PINK1, including the mitochondrial fusion protein Marf (Liu and Lu 2010; Ziviani et al. 2010), the autophagy regulator Atg1 (Liu and Lu 2010), and the mitochondrial transport protein Miro (Wang et al. 2011; Liu et al. 2012). Marf RNAi or Atg1 GOF effectively blocked the enhancing effects of mTORC2 LOF (Fig. 4I,J) or Trc LOF (Fig. 4K,L) in the *dPINK1* mutant background. Miro RNAi was also effective, although to a lesser degree (Fig. 4I–L). Together, these genetic epistasis data support critical roles of mTORC2 and Trc in mediating the effect of PINK1 in MQC and tissue maintenance.

In mammalian cells, the PINK1–Parkin pathway also plays central roles in MQC, with Parkin recruited to damaged mitochondria in a PINK1-dependent manner to promote mitophagy (Narendra et al. 2010). We tested whether the mammalian Trc homologs NDR1/2 act in PINK1/Parkin-directed MQC. Knockdown of NDR1 but not NDR2 in HeLa cells led to altered mitochondrial distribution, compromised recruitment of Parkin by PINK1, and delayed clearance of damaged mitochondria (Supplemental Fig. S9A–C). The mitophagy defects induced by NDR1 RNAi were rescued by a siRNA-resistant NDR1 construct (Supplemental Fig. S9B,D). Importantly, we detected reduced phosphorylation of NDR1 at the corresponding T444 site in *PINK1*$^{-/-}$ mouse embryonic fibroblasts (MEFs) expressing a kinase-dead form of PINK1 but not wild-type PINK1 (Supplemental Fig. S10). Due to the hypersensitivity of p-NDR1 to endogenous phosphatase activities as previously reported (Koike-Kumagai et al. 2009), treatment with okadaic acid (OA) was needed to reveal the effect of PINK1 on the p-NDR1 level. These results support that NDR1 acts in the PINK1/Parkin pathway in mammals. In carbonyl cyanide m-chlorophe-

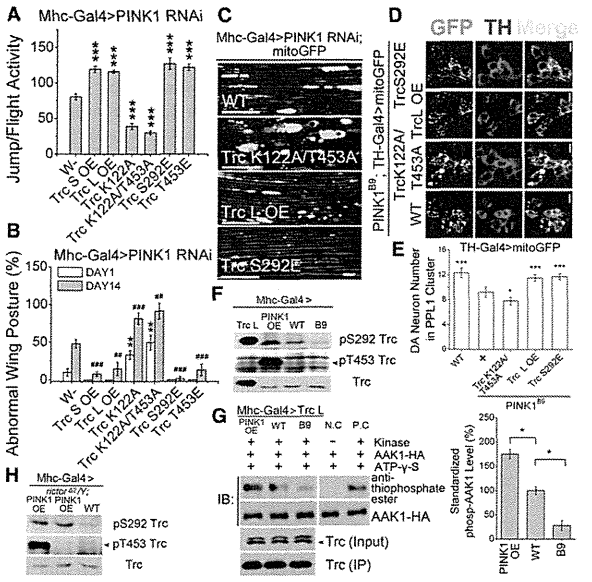

Figure 3. Evidence that Trc acts in the PINK1 pathway. (*A,B*) *Mhc-Gal4>PINK1 RNAi*-induced flight ability (*A*) and wing posture (*B*) defects were rescued by the coexpression of the short (S) or long (L) isoforms of wild-type Trc or constitutively active (S292E or T453E) Trc but enhanced by dominant-negative (K122A or K122A/T453A) Trc. (* or #) $P < 0.05$; (** or ##) $P < 0.01$; (*** or ###) $P < 0.005$ in one-way ANOVA tests when data from day 1 (*) or day 14 (#) were compared. (*C*) *Mhc-Gal4>PINK1 RNAi*-induced mitochondrial aggregation in indirect flight muscle was rescued by the coexpression of Trc-L or Trc-S292E but enhanced by Trc-K122A/T453A. Mitochondrial morphology was monitored with a mito-GFP reporter. Bar, 30 μm. (*D,E*) *PINK1*^{B9} mutation-induced mitochondrial aggregation in DNs (*D*) or loss of DNs in the PPL1 clusters (*E*) was strongly rescued by *TH-Gal4*-driven expression of wild-type or constitutively active Trc but enhanced by dominant-negative Trc. Bar, 5 μm. (*F*) Western blot analysis showing the effects of PINK1 LOF or overexpression on Trc phosphorylation. Trc-L overexpression served as a positive control. (*G*) In vitro kinase assay showing the effects of PINK1 LOF or overexpression on Trc kinase activity. Trc-L purified from control, PINK1 mutant, and PINK1-overexpressing animals was tested for kinase activity using AAK1-HA as a substrate in the presence of ATP-γ-S and phosphorylation detected by anti-thiophosphate ester antibody after esterification with p-nitrobenzylmesylate (PNBM). (P.C.) Positive control with extract added; (N.C.) negative control with no kinase added. Bar graph shows data quantification. (*H*) Western blot analysis showing that PINK1-induced Trc phosphorylation of T453 was Rictor-dependent, whereas that of S292 was Rictor-independent. (*) $P < 0.05$; (***) $P < 0.005$ in one-way ANOVA tests in *E* and *G*.

nylhydrazone (CCCP)-treated HeLa cells, NDR1 was found to colocalize with Parkin and the mitochondrial outer membrane marker Tom 20 (Supplemental Fig. S9B), suggesting that NDR1 might also be localized to mitochondria to exert MQC. In Parkin stably transfected HeLa cells that were subjected to Rictor RNAi (Supplemental Fig. S11A,D) or in *rictor*$^{-/-}$ MEF cells (Supplemental Fig. S11B,C,E), the recruitment of Parkin to damaged mitochondria and the kinetics of mitophagy were also delayed, supporting a critical role of mTORC2 in PINK1/Parkin-directed mitophagy in mammals.

We further investigated the mechanism of action of NDR1 in mammalian cells. It has been reported that Parkin is phosphorylated and activated by phosphorylation upon CCCP treatment (Kondapalli et al. 2012; Shiba-Fukushima et al. 2012). In HeLa cells stably transfected with Parkin, CCCP treatment led to increased phosphorylation of NDR1 and Parkin as detected with Phos tag. NDR1 RNAi significantly attenuated Parkin phosphorylation (Supplemental Fig. S12A), consistent with Parkin acting downstream from NDR1. Further supporting this notion, the activity of Parkin as measured by its autoubiquitination was reduced by NDR1 RNAi (Supplemental Fig. S12B). Moreover, the destabilization of MQC-related proteins Mfn1 and Miro1 by CCCP-activated PINK1/Parkin signaling was significantly attenuated by NDR1 RNAi (Supplemental Fig. S12A). These results support the notion that, as in flies, NDR1 kinase signaling acts upstream of Parkin and the other key MQC players in the mammalian MQC pathway.

Our results demonstrate that mTORC2 and Trc signaling are actively involved in the dynamic MQC network directed by PINK1 and that they act between PINK1 and Parkin in a conserved signaling pathway. This finding reveals a previously unappreciated complexity in the signaling steps between PINK1 and Parkin. This is the first time both mTORC2 and Trc are directly implicated in MQC. The fact that PINK1 regulates Trc T453 phosphorylation in an mTORC2-dependent manner and S292 phosphorylation in an mTORC2-independent manner suggests the involvement of additional kinases in this MQC pathway. Our finding of active p-Trc localizing primarily to mitochondria suggests that mitochondria may serve as a key platform for Trc signaling. The kinase that directly acts on Trc T453 in the context studied here remains to be identified. Although mTORC2 is required, it may not be the kinase that directly phosphorylates this site (Koike-Kumagai et al. 2009). Similarly, although PINK1 is required for mTORC2 activation, our results suggest that PINK1 acts through maintaining mitochondrial CI activity to influence mTORC2 activity, rather than directly phosphorylating mTORC2 as proposed in a previous study (Murata et al. 2011). Our findings offer new insights into the novel role of mitochondria in regulating mTORC2 and Trc/NDR kinase signaling.

mTORC2 and Trc signaling both induce cell morphology changes through actin cytoskeleton regulation (Jacinto et al. 2004; Fang and Adler 2010). Given the dynamic changes in mitochondrial distribution and morphology during MQC and the implicated roles of the actin cytoskeleton in regulating mitochondrial distribution and morphology (Boldogh and Pon 2006), it is possible that mTORC2/Trc may act in MQC through cytoskeletal regulation, although this remains to be tested. Our results support the notion that Trc signaling directly impinges on Parkin or the other key MQC executors (Supplemental Fig. S12C). A corollary of our finding is that mitochondrial localization of the kinases and the ensuing MQC may participate in other physiological processes regulated by mTORC2/Trc signaling. Given that deregulated mTORC2 (Zoncu et al. 2011), Trc/NDR (Cornils et al. 2011), and PINK1 and Parkin (Devine et al. 2011) signaling have all been linked to cancer in humans, another important implication of this study is that aberrant MQC signaling also contributes to cancerous growth and that therapeutic agents targeting the newly identified, highly conserved MQC signaling pathway may have broad therapeutic applications.

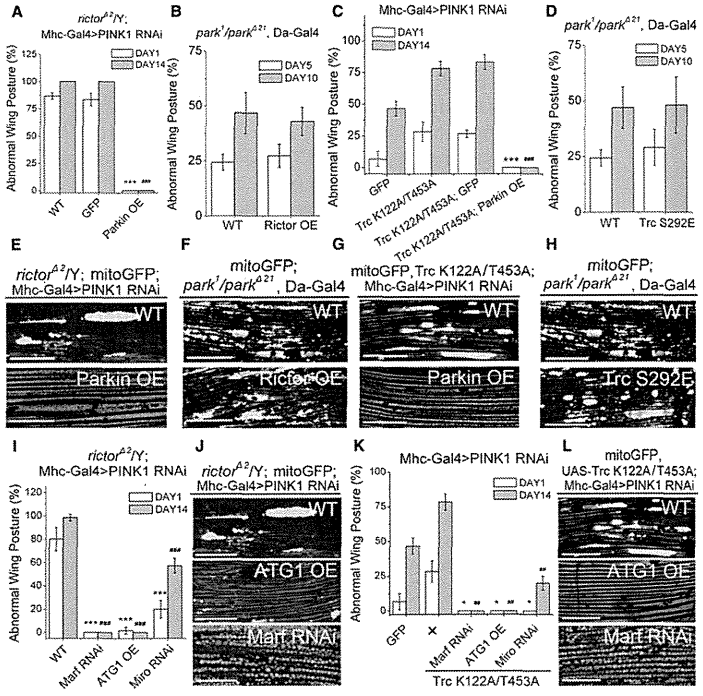

Figure 4. Genetic evidence that Parkin and MQC executors act downstream from TORC2 and Trc in the PINK1 pathway. (*A*,*E*) The enhancement of PINK1 RNAi-induced abnormal wing posture (*A*) or mitochondrial aggregation (*E*) by *rictor* deletion was suppressed by Parkin but not GFP overexpression. (*B*,*F*) The rescue of PINK1 RNAi-induced abnormal wing posture (*B*) or mitochondrial aggregation (*F*) by Rictor overexpression was blocked by Parkin LOF. (*C*,*G*) The enhancement of PINK1 RNAi-induced abnormal wing posture (*C*) or mitochondrial aggregation (*G*) by dominant-negative Trc was completely suppressed by Parkin but not GFP overexpression. (*D*,*H*) The rescue of PINK1 RNAi-induced abnormal wing posture (*D*) or mitochondrial aggregation (*H*) by wild-type or constitutively active Trc was blocked by Parkin LOF. (*I*,*J*) The enhancement of PINK1 RNAi-induced abnormal wing posture (*I*) or mitochondrial aggregation (*J*) by *rictor* deletion was suppressed by Miro-RNAi, Marf-RNAi, or Atg1 overexpression. (*K*,*L*) The enhancement of PINK1 RNAi-induced abnormal wing posture by dominant-negative Trc was suppressed by Miro-RNAi, Marf-RNAi, or Atg1 overexpression. (* or #) $P < 0.05$; (** or ##) $P < 0.01$; and (*** or ###) $P < 0.005$ in one-way ANOVA or Student's *t*-tests when data from day 1 (*) or day 14 (#) were compared. Bars: *E–F*,*J*,*L*, 30 μm.

Materials and methods

GST fusion protein preparation

The construct expressing human GST-AKT-KD used as the substrate in the in vitro TORC2 kinase assays was a gift from Dr. Dianqing Wu. To avoid autophosphorylation of AKT, the Lys179 and Thr308 residues were mutated (Gan et al. 2011). GST fusion protein was expressed in the *Escherichia coli BL21 (DE3)* strain and purified using glutathione-agarose beads following standard protocols.

Immunoprecipitation and kinase assay of TORC2

For TORC2 immunoprecipitation, methods adopted from previous studies (Koike-Kumagai et al. 2009; Gan et al. 2011) were used. Briefly, flies were crossed and raised in standard medium at 25°C. Male flies expressing Flag-tagged Sin1 were collected and homogenized in lysis buffer (40 mM HEPES at pH 7.5, 120 mM NaCl, 0.3% CHAPS, 1 mM EDTA, 10 mM β-glycerophosphate, 50 mM NaF, 1 mM PMSF). TORC2 was immunoprecipitated by incubating the supernatant with pre-equilibrated anti-Flag M2 beads (Sigma Aldrich) for 3 h at 4°C. Immunocomplexes were washed 3 times in lysis buffer and twice with the TORC2 kinase buffer (25 mM HEPES at pH 7.5, 100 mM KAc, 2 mM $MgCl_2$). The integrity of the TORC2 was confirmed by Western blot analysis.

For kinase assays, TORC2 immunocomplexes were incubated with 500 ng of human GST-AKT-KD fusion protein in 30 μL of TORC2 kinase buffer containing 500 μM ATP. The reaction was performed for 30 min at 30°C and terminated by the addition of 30μL of 2× SDS sample buffer. AKT phosphorylation by TORC2 was analyzed by Western blot using the p-T473-AKT antibody (Cell Signaling Technology).

Mitochondrial and cytoplasmic protein fractionation

For mitochondria purification, we adopted a previous method (Kristian et al. 2006). Briefly, fly tissues were collected and homogenized in homogenization buffer (210 mM mannitol, 70 mM sucrose, 1 mM EGTA, 10 mM β-glycerophosphate, 50 mM NaF, 1 mM PMSF, 5 mM HEPES at pH 7.12). The homogenate was centrifuged at 1500*g* for 5 min, and the supernatant was collected and centrifuged again at 13,000*g* for 17 min. The supernatant was concentrated as a cytoplasmic protein sample, and the pellet was stored for further mitochondrial purification. For mitochondrial purification, the previous pellet was resuspended in 15% Percoll solution and loaded onto a 15%–22%–50% discontinuous Percoll gradient. The gradient was centrifuged at 30,700*g* for 6 min, and intact mitochondria were recovered from the 22%–50% gradient interface. Mitochondria were washed with homogenization buffer and subjected to SDS-PAGE.

Quantitative Western blot analysis

To obtain quantitative Western blot results, experimental conditions such as the amounts of protein loaded, the antibody dilutions, and exposure times were adjusted to make sure that the Western blot signals were in the linear range. For the in vitro kinase assays, Western blot analyses were performed using standard protocols. After incubation with the ECL reagent (PerkinElmer, Inc.), the signals were scanned using a Typhoon 9400 system (GE Healthcare Life Sciences), and signal intensity was quantified by ImageQuantTL. For the other immunoblots, the signals were recorded on X-ray film and scanned, and the signal intensity was analyzed by ImageQuantTL or ImageJ. Statistical analyses were based on data from three independent repeats.

Statistical analysis

Two-tailed Student's *t*-tests were used in the statistical analysis when comparing two samples. A one-way ANOVA test was used when multiple samples were compared.

Acknowledgments

We thank Dr. P. Aspenström, Dr. E. Baehrecke, Dr. R. Baloh, Dr. S. Birman, Dr. J. Chung, Dr. S. Cohen, Dr. K. Emoto, Dr. M. Guo, Dr. Y. Hata, Dr. S. Hatakeyama, Dr. B. Hemmings, Dr. Y.N. Jan, Dr. S. Konur, Dr. M. Magnuson, Dr. N. Matsuda, Dr. K. Nakagawa, Dr. W. Saxton, Dr. K. Tanaka, Dr. G. Thomas, Dr. P. Verstreken, Dr. D. Wu, Dr. K. Zinsmaier, Bloomington *Drosophila* Stock Center, Vienna *Drosophila* RNAi Center, and TRiP at Harvard Medical School (NIH/NIGMS R01-GM084947) for flies and reagents, and Lu laboratory members for technical help and discussions. This work was supported by the NIH (R01AR054926 and R01MH080378 to B.L.), Grant-in-Aid for Young Scientists (B) from MEXT in Japan (to Y.I.), the CREST program of JST (to R.T.), a Grant-in-Aid for Scientific Research on Innovative Areas (to R.T.), and a Grant-in-Aid for Science Research from the Ministry of Health, Labor, and Welfare in Japan (to R.T.).

References

Boldogh IR, Pon LA. 2006. Interactions of mitochondria with the actin cytoskeleton. *Biochim Biophys Acta* **1763:** 450–462.

Clark IE, Dodson MW, Jiang C, Cao JH, Huh JR, Seol JH, Yoo SJ, Hay BA, Guo M. 2006. *Drosophila* pink1 is required for mitochondrial function and interacts genetically with parkin. *Nature* **441:** 1162–1166.

Cornils H, Kohler RS, Hergovich A, Hemmings BA. 2011. Downstream of human NDR kinases: Impacting on c-myc and p21 protein stability to control cell cycle progression. *Cell Cycle* **10:** 1897–1904.

Devine MJ, Plun-Favreau H, Wood NW. 2011. Parkinson's disease and cancer: Two wars, one front. *Nat Rev Cancer* **11:** 812–823.

Emoto K, He Y, Ye B, Grueber WB, Adler PN, Jan LY, Jan YN. 2004. Control of dendritic branching and tiling by the Tricornered-kinase/Furry signaling pathway in *Drosophila* sensory neurons. *Cell* **119:** 245–256.

Emoto K, Parrish JZ, Jan LY, Jan YN. 2006. The tumour suppressor Hippo acts with the NDR kinases in dendritic tiling and maintenance. *Nature* **443:** 210–213.

Exner N, Treske B, Paquet D, Holmström K, Schiesling C, Gispert S, Carballo-Carbajal I, Berg D, Hoepken HH, Gasser T, et al. 2007. Loss-of-function of human PINK1 results in mitochondrial pathology and can be rescued by parkin. *J Neurosci* **27:** 12413–12418.

Fang X, Adler PN. 2010. Regulation of cell shape, wing hair initiation and the actin cytoskeleton by Trc/Fry and Wts/Mats complexes. *Dev Biol* **341:** 360–374.

Gan X, Wang J, Su B, Wu D. 2011. Evidence for direct activation of mTORC2 kinase activity by phosphatidylinositol 3,4,5-trisphosphate. *J Biol Chem* **286:** 10998–11002.

Geng W, He B, Wang M, Adler PN. 2000. The tricornered gene, which is required for the integrity of epidermal cell extensions, encodes the Drosophila nuclear DBF2-related kinase. *Genetics* **156:** 1817–1828.

Hergovich A, Stegert MR, Schmitz D, Hemmings BA. 2006. NDR kinases regulate essential cell processes from yeast to humans. *Nat Rev Mol Cell Biol* **7:** 253–264.

Hietakangas V, Cohen SM. 2007. Re-evaluating AKT regulation: Role of TOR complex 2 in tissue growth. *Genes Dev* **21:** 632–637.

Jacinto E, Loewith R, Schmidt A, Lin S, Ruegg MA, Hall A, Hall MN. 2004. Mammalian TOR complex 2 controls the actin cytoskeleton and is rapamycin insensitive. *Nat Cell Biol* **6:** 1122–1128.

Kitada T, Asakawa S, Hattori N, Matsumine H, Yamamura Y, Minoshima S, Yokochi M, Mizuno Y, Shimizu N. 1998. Mutations in the parkin gene cause autosomal recessive juvenile parkinsonism. *Nature* **392:** 605–608.

Koike-Kumagai M, Yasunaga K, Morikawa R, Kanamori T, Emoto K. 2009. The target of rapamycin complex 2 controls dendritic tiling of *Drosophila* sensory neurons through the Tricornered kinase signalling pathway. *EMBO J* **28:** 3879–3892.

Kondapalli C, Kazlauskaite A, Zhang N, Woodroof HI, Campbell DG, Gourlay R, Burchell L, Walden H, Macartney TJ, Deak M, et al. 2012. PINK1 is activated by mitochondrial membrane potential depolarization and stimulates Parkin E3 ligase activity by phosphorylating Serine 65. *Open Biol* **2:** 120080.

Kristian T, Hopkins IB, McKenna MC, Fiskum G. 2006. Isolation of mitochondria with high respiratory control from primary cultures of neurons and astrocytes using nitrogen cavitation. *J Neurosci Methods* **152:** 136–143.

Liu S, Lu B. 2010. Reduction of protein translation and activation of autophagy protect against PINK1 pathogenesis in *Drosophila melanogaster*. *PLoS Genet* **6:** e1001237.

Liu W, Acín-Peréz R, Geghman KD, Manfredi G, Lu B, Li C. 2011. Pink1 regulates the oxidative phosphorylation machinery via mitochondrial fission. *Proc Natl Acad Sci* **108:** 12920–12924.

Liu S, Sawada T, Lee S, Yu W, Silverio G, Alapatt P, Millan I, Shen A, Saxton W, Kanao T, et al. 2012. Parkinson's disease-associated kinase PINK1 regulates miro protein level and axonal transport of mitochondria. *PLoS Genet* **8:** e1002537.

Murata H, Sakaguchi M, Jin Y, Sakaguchi Y, Futami J, Yamada H, Kataoka K, Huh NH. 2011. A new cytosolic pathway from a Parkinson disease-associated kinase, BRPK/PINK1: Activation of AKT via mTORC2. *J Biol Chem* **286:** 7182–7189.

Narendra DP, Youle RJ. 2011. Targeting mitochondrial dysfunction: Role for PINK1 and Parkin in mitochondrial quality control. *Antioxid Redox Signal* **14:** 1929–1938.

Narendra DP, Jin SM, Tanaka A, Suen DF, Gautier CA, Shen J, Cookson MR, Youle RJ. 2010. PINK1 is selectively stabilized on impaired mitochondria to activate Parkin. *PLoS Biol* **8:** e1000298.

Park J, Lee SB, Lee S, Kim Y, Song S, Kim S, Bae E, Kim J, Shong M, Kim JM, et al. 2006. Mitochondrial dysfunction in *Drosophila* PINK1 mutants is complemented by parkin. *Nature* **441:** 1157–1161.

Rugarli EI, Langer T. 2012. Mitochondrial quality control: A matter of life and death for neurons. *EMBO J* **31:** 1336–1349.

Russell RC, Fang C, Guan KL. 2011. An emerging role for TOR signaling in mammalian tissue and stem cell physiology. *Development* **138:** 3343–3356.

Sarbassov DD, Guertin DA, Ali SM, Sabatini DM. 2005. Phosphorylation and regulation of Akt/PKB by the rictor–mTOR complex. *Science* **307:** 1098–1101.

Shiba-Fukushima K, Imai Y, Yoshida S, Ishihama Y, Kanao T, Sato S, Hattori N. 2012. PINK1-mediated phosphorylation of the Parkin ubiquitin-like domain primes mitochondrial translocation of Parkin and regulates mitophagy. *Sci Rep* **2:** 1002.

Ultanir SK, Hertz NT, Li G, Ge WP, Burlingame AL, Pleasure SJ, Shokat KM, Jan LY, Jan YN. 2012. Chemical genetic identification of NDR1/2 kinase substrates AAK1 and Rabin8 uncovers their roles in dendrite arborization and spine development. *Neuron* **73:** 1127–1142.

Valente EM, Abou-Sleiman PM, Caputo V, Muqit MM, Harvey K, Gispert S, Ali Z, Del Turco D, Bentivoglio AR, Healy DG, et al. 2004. Hereditary early-onset Parkinson's disease caused by mutations in PINK1. *Science* **304:** 1158–1160.

Vilain S, Esposito G, Haddad D, Schaap O, Dobreva MP, Vos M, Van Meensel S, Morais VA, De Strooper B, Verstreken P. 2012. The yeast complex I equivalent NADH dehydrogenase rescues pink1 mutants. *PLoS Genet* **8:** e1002456.

Wang X, Winter D, Ashrafi G, Schlehe J, Wong YL, Selkoe D, Rice S, Steen J, Lavoie MJ, Schwarz TL. 2011. PINK1 and Parkin target miro for phosphorylation and degradation to arrest mitochondrial motility. *Cell* **147:** 893–906.

Wullschleger S, Loewith R, Hall MN. 2006. TOR signaling in growth and metabolism. *Cell* **124:** 471–484.

Yang Y, Gehrke S, Imai Y, Huang Z, Ouyang Y, Wang JW, Yang L, Beal MF, Vogel H, Lu B. 2006. Mitochondrial pathology and muscle and dopaminergic neuron degeneration caused by inactivation of *Drosophila* Pink1 is rescued by Parkin. *Proc Natl Acad Sci* **103:** 10793–10798.

Yang Y, Ouyang Y, Yang L, Beal MF, McQuibban A, Vogel H, Lu B. 2008. Pink1 regulates mitochondrial dynamics through interaction with the fission/fusion machinery. *Proc Natl Acad Sci* **105:** 7070–7075.

Ziviani E, Tao RN, Whitworth AJ. 2010. *Drosophila* parkin requires PINK1 for mitochondrial translocation and ubiquitinates Mitofusin. *Proc Natl Acad Sci* **107:** 5018–5023.

Zoncu R, Efeyan A, Sabatini DM. 2011. mTOR: From growth signal integration to cancer, diabetes and ageing. *Nat Rev Mol Cell Biol* **12:** 21–35.

Tricornered/NDR kinase signaling mediates PINK1-directed mitochondrial quality control and tissue maintenance

Zhihao Wu, Tomoyo Sawada, Kahori Shiba, et al.

Genes Dev. 2013 27: 157-162
Access the most recent version at doi:10.1101/gad.203406.112

Neurobiology of Aging 35 (2014) 1779.e17–1779.e21

Contents lists available at ScienceDirect

Neurobiology of Aging

journal homepage: www.elsevier.com/locate/neuaging

The evaluation of polyglutamine repeats in autosomal dominant Parkinson's disease

Chikara Yamashita [a], Hiroyuki Tomiyama [a,b], Manabu Funayama [a,c], Saeko Inamizu [d], Maya Ando [a], Yuanzhe Li [c], Hiroyo Yoshino [c], Takehisa Araki [d], Tadashi Ichikawa [e], Yoshiro Ehara [f], Kinya Ishikawa [g], Hidehiro Mizusawa [g], Nobutaka Hattori [a,b,c,*]

[a] Department of Neurology, Graduate School of Medicine, Juntendo University, Bunkyo-ku, Tokyo, Japan
[b] Department of Neuroscience for Neurodegenerative Disorders, Graduate School of Medicine, Juntendo University, Bunkyo-ku, Tokyo, Japan
[c] Research Institute for Diseases of Old Age, Graduate School of Medicine, Juntendo University, Bunkyo-ku, Tokyo, Japan
[d] Department of Neurology, Hiroshima Red Cross Hospital & Atomic-bomb Survivors Hospital, Naka-ku, Hiroshima, Japan
[e] Department of Neurology, Saitama Prefectural Rehablitation Center, Ageo-city, Saitama, Japan
[f] Department of Medical Education, Graduate School of Medicine, Juntendo University, Bunkyo-ku, Tokyo, Japan
[g] Department of Neurology and Neurological Science, Graduate School of Medical and Dental Sciences, Tokyo Medical and Dental University, Bunkyo-ku, Tokyo, Japan

ARTICLE INFO

Article history:
Received 9 January 2013
Received in revised form 20 January 2014
Accepted 21 January 2014
Available online 25 January 2014

Keywords:
Trinucleotide repeat diseases
Parkinson's disease
Polyglutamine
Intermediate length
Ataxin-2

ABSTRACT

We evaluated the contributions of various polyglutamine (polyQ) disease genes to Parkinson's disease (PD). We compared the distributions of polyQ repeat lengths in 8 common genes (*ATXN1*, *ATXN2*, *ATXN3*, *CACNA1A*, *ATXN7*, *TBP*, *ATN1*, and *HTT*) in 299 unrelated patients with autosomal dominant PD (ADPD) and 329 normal controls. We also analyzed the possibility of genetic interactions between *ATXN1* and *ATXN2*, *ATXN2* and *ATXN3*, and *ATXN2* and *CACNA1A*. Intermediate-length polyQ expansions (>24 Qs) of *ATXN2* were found in 7 ADPD patients and no controls (7/299 = 2.34% and 0/329 = 0%, respectively; $p = 0.0053 < 0.05/8$ after Bonferroni correction). These patients showed typical L-DOPA-responsive PD phenotypes. Conversely, no significant differences in polyQ repeat lengths were found between the ADPD patients and the controls for the other 7 genes. Our results may support the hypothesis that *ATXN2* polyQ expansion is a specific predisposing factor for multiple neurodegenerative diseases.

1. Introduction

Several genes other than the "PARK" genes are suspected to be responsible for parkinsonism. Mutations of these genes sometimes confer symptoms that clinically mimic idiopathic Parkinson's disease (PD) and present radiological or pathologic findings characteristic of PD (Klein et al., 2009). These genes include the polyglutamine (polyQ) disease genes: *HTT* (Walker, 2007), *ATXN1* (Dubourg et al., 1995), *ATXN2* (Charles et al., 2007; Furtado et al., 2004; Gwinn-Hardy et al., 2000), *ATXN3* (Lu et al., 2004a; Subramony et al., 2002), *CACNA1A* (Kim et al., 2010), and *TBP* (Kim et al., 2009). Of these genes, it has been suggested that intermediate-length polyQ expansions in *ATXN2* and *TBP* are associated with PD (Charles et al., 2007; Furtado et al., 2004; Kim et al., 2009).

In addition, intermediate-length polyQ expansions (24–33 Qs) in *ATXN2* have recently been suggested as a risk factor for amyotrophic lateral sclerosis (ALS) (Chen et al., 2011; Elden et al., 2010). This observation has inspired several studies investigating how intermediate-length expansions of various polyQ disease genes contribute to neurodegenerative diseases other than those with which they were originally associated (Gispert et al., 2012; Lee et al., 2011b; Ross et al., 2011).

Based on these findings and the suggestion that polyQ diseases may share common pathogenic mechanisms (Al-Ramahi et al., 2007; Bertoni et al., 2011; Chen and Burgoyne, 2012), we hypothesized that polyQ disease genes in general might play a role in PD. We focused on autosomal dominant PD (ADPD) because polyQ neurodegenerative diseases generally have an AD mode of inheritance, and we compared the distribution of polyQ repeat lengths in 8 common genes between ADPD patients and normal controls.

2. Methods

We conducted genetic analyses of *ATXN1*, *ATXN2*, *ATXN3*, *CACNA1A*, *ATXN7*, *TBP*, *ATN1*, and *HTT* in a Japanese cohort with ADPD and normal controls. In this study, we classified the mode of

* Corresponding author at: Department of Neurology and Department of Neuroscience for Neurodegenerative Disorders, Graduate School of Medicine, Juntendo University, 2-1-1 Hongo, Bunkyo-ku, Tokyo 113-8421, Japan. Tel.: +81 3 5802 1073; fax: +81 3 5800 0547.
E-mail address: nhattori@juntendo.ac.jp (N. Hattori).

0197-4580/$ – see front matter © 2014 Elsevier Inc. All rights reserved.
http://dx.doi.org/10.1016/j.neurobiolaging.2014.01.022

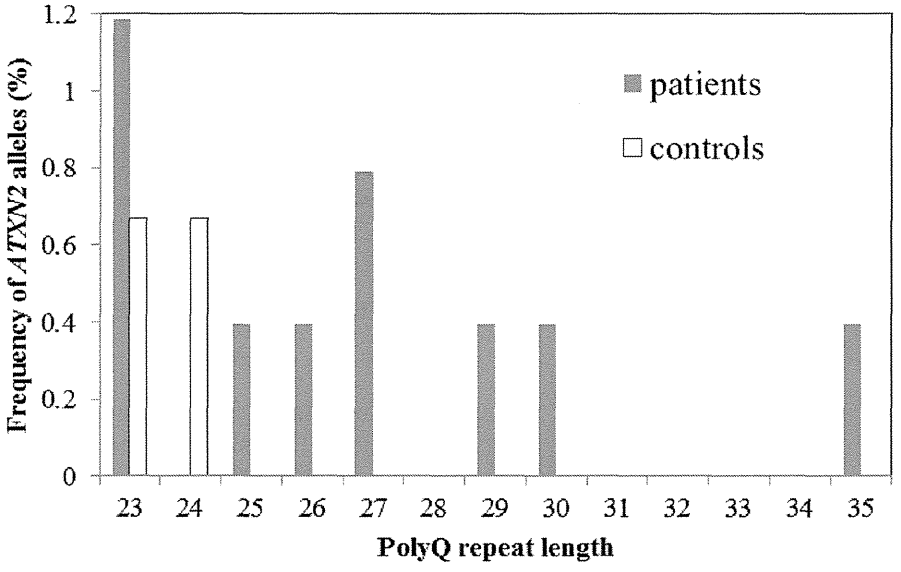

PolyQ length	19	20-21	22	23	24	25	26	27	28	29	30	31-34	35
Patients	1	0	288	3	0	1	1	2	0	1	1	0	1
Controls	0	0	325	2	2	0	0	0	0	0	0	0	0

Fig. 1. The distribution of polyglutamine (polyQ) repeat lengths of *ATXN2* in autosomal dominant Parkinson's disease patients and normal controls. The histogram shows only subjects with ≥23 repeats.

inheritance as autosomal dominant when a family included affected members in 2 consecutive generations. The diagnosis of PD was confirmed by the participating neurologists based on established criteria (Hughes et al., 1992).

We recruited the study subjects from the gene bank of our institution. We selected 299 unrelated patients with ADPD (169 women and 130 men; age at onset [AAO] = 57.7 ± 13.6-year-old [standard deviation], range 17–85 years) from families with unexplained pathogenesis, that is, those with no known pathogenic mutations in the *SNCA*, *PARK2*, *LRRK2*, and *VPS35* genes. A total of 329 healthy unrelated volunteers with no individual or family history of neurodegenerative disease (203 women and 126 men; age at examination = 57.5 ± 11.8-year-old [standard deviation], range 23–88 years) were examined as normal controls. Blood samples were obtained from the patients and controls, all of whom gave informed consent. Our institutional ethics committee approved the genetic study.

DNA was extracted from lymphocytes using standard methods. The polyQ repeat lengths in the polyQ disease genes were detected using capillary electrophoresis with fluorescent 5′-6-fluorescein amidite (FAM)-labeled forward primers. The primer sequences and polymerase chain reaction conditions are described in Supplementary Table 1. The polymerase chain reaction products were mixed with the LIZ-500 size standard (Applied Biosystems, Foster City, CA, USA) and processed on an Applied Biosystems 3130 Genetic Analyzer (Applied Biosystems) for size determination. The sizes of the repeats were determined with GeneMapper 3.7 software (Applied Biosystems).

Statistical analysis was performed using JMP 8 software (SAS Institute, Cary, NC, USA). We evaluated the association between ADPD and the polyQ repeat lengths of each gene using 2-tailed Fisher exact tests, as previously described (Gispert et al., 2012; Lee et al., 2011a; Ross et al., 2011). A p value <0.05/8 after Bonferroni correction was considered significant (8 is for the number of genes investigated in the present study.).

3. Results

3.1. Molecular genetic analysis

The range of repeat lengths in *ATXN2* was between 19 and 35. Most patients (95.6% of patients with ADPD and 98.6% of the controls) had a repeat length of 22, as reported in previous studies (Lee et al., 2011a; Pulst et al., 1996). Of the 253 patients with ADPD, 7 harbored repeat lengths longer than 24, whereas none of the controls did (2.8% and 0%, respectively; $p = 0.0053$, Fig. 1 and Table 1).

No substantial differences in the repeat lengths in *ATXN1*, *ATXN3*, *CACNA1A*, *ATXN7*, *TBP*, *ATN1*, or *HTT* were observed between the ADPD patients and controls (Table 1 and Supplementary Fig. 1).

We supplementarily sequenced the entire coding exons and exon and/or intron boundaries of glucocerebrosidase gene (*GBA*) in

Table 1
Fisher exact tests of polyQ repeat lengths between ADPD patients and controls

PolyQ disease gene	PolyQ repeat length	Conventional normal range[a]	Difference between ADPD patients and controls?
ATXN1	21–36 19–35	6–44	No
ATXN2	25–35Qs: 2.3% of ADPD, 0% of control	14–31	Yes, $p = 0.0053$ (<0.05/8), OR = ∞
ATXN3	13–46	11–44	No
CACNA1A	5–18	4–18	No
ATXN7	1–10	4–19	No
TBP	30–40	25–42	No
ATN1	12–36	6–35	No
HTT	15–35	6–34	No

Key: ADPD, autosomal dominant Parkinson's disease; Q, glutamine.
[a] The consensus normal ranges of the polyQ repeat lengths associated with the corresponding disease (e.g., *ATXN1* for SCA1) (Hands et al., 2008; Sequeiros et al., 2010).

the 7 probands with intermediate *ATXN2* polyQ expansion, because rare *GBA* mutations have been considered to be a risk factor for PD (Li et al., 2013; Mitsui et al., 2009); no *GBA* mutation was found in these 7 probands.

3.2. Pedigree and clinical information for the 7 probands with ATXN2 polyQ repeat lengths >24

Fig. 2 shows the pedigrees of the 7 probands with *ATXN2* polyQ repeat lengths >24 and their families. In family A, AII-2 presented with resting tremor in the bilateral lower extremities and left-dominant bradykinesia, which were responsive to L-DOPA and selegiline. AIII-1, who experienced rigidity and resting tremor predominantly in the left extremities, presented with tongue and jaw tremor (Supplementary Table 2). All these signs were relieved by pramipexole. AIII-3 was reportedly initially diagnosed with essential tremor because her first sign was bilateral postural tremor. She underwent left and right thalamotomy at a 1-year interval. She showed hyperreflexia in the lower extremities, but this symptom was presumably because of cervical spondylosis, for which surgical decompression was performed. AIV-2 and AIV-3, who inherited an intermediate-length polyQ expansion of 35 Qs, were not affected at the time of this study.

In family B, BI-2 was affected at an older age than her offspring, although their genotypes were the same, and all had L-DOPA-responsive parkinsonism with laterality (Supplementary Table 2).

In family C, CII-2 was diagnosed with Parkinson's disease with dementia. Although her parents were consanguineous, her polyQ *ATXN2* lengths were heterozygous (29/22).

All other members of the 7 families showed L-DOPA-responsive parkinsonism with laterality and were free of motor neuron signs, cerebellar ataxia, and saccadic eye movement disorder. None was

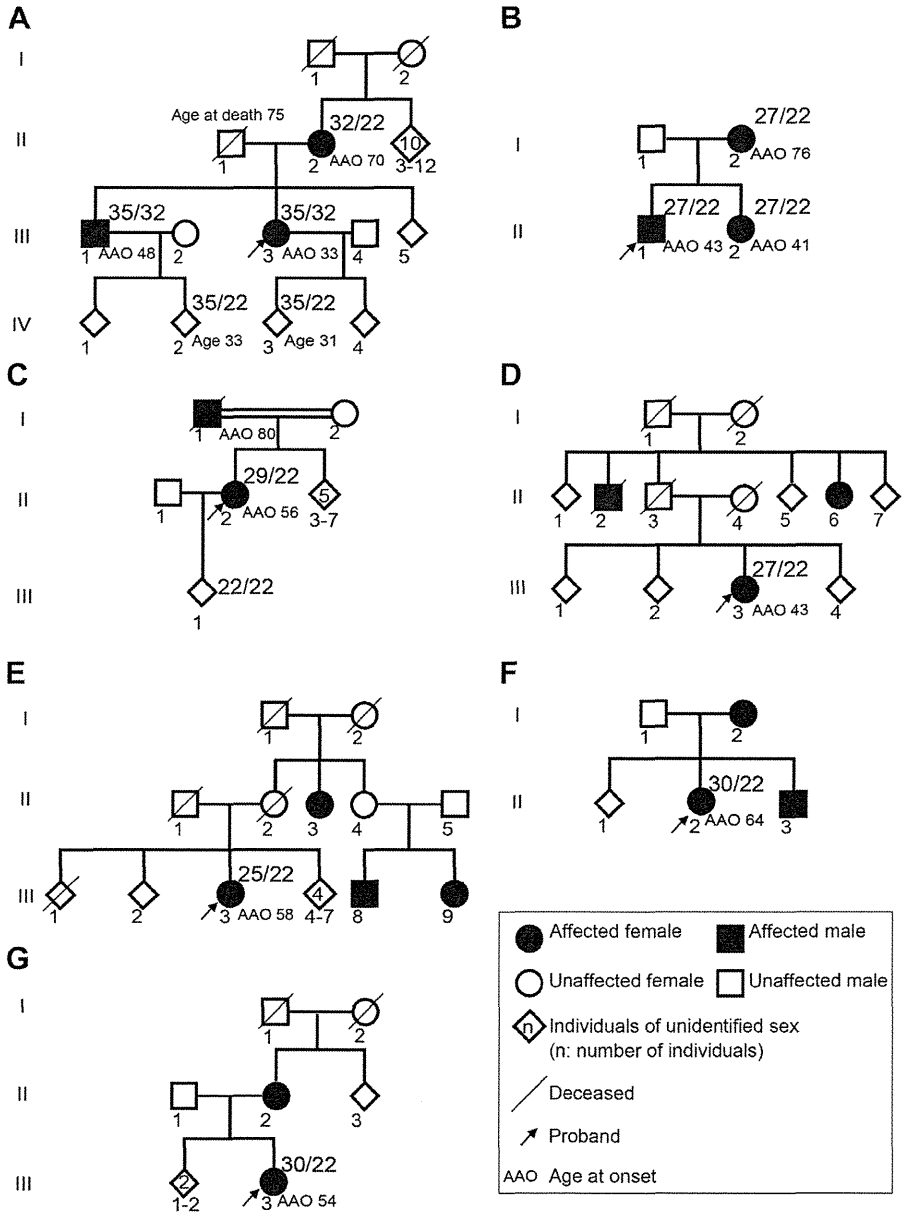

Fig. 2. The pedigrees of 7 families in which the proband has an *ATXN2* polyQ repeat length >24. *ATXN2* repeat lengths are listed previously and to the right of the pedigree symbols of the genotyped individuals.

reported to have any significant brain magnetic resonance imaging abnormality (Supplementary Table 2).

4. Discussion

We investigated the distributions of the polyQ repeat lengths of 8 common polyQ disease genes (*ATXN1*, *ATXN2*, *ATXN3*, *CACNA1A*, *ATXN7*, *TBP*, *ATN1*, and *HTT*) in patients with ADPD. PolyQ repeat lengths >24 in *ATXN2* were significantly more common in the patients than in the controls. To the best of our knowledge, there have been only 2 similar studies investigating the distribution of *ATXN2* polyQ repeat lengths in PD patients and controls to date (Gispert et al., 2012; Ross et al., 2011). Although both previous studies failed to prove any significant difference, one (Gispert et al., 2012) showed that PD patients tended to have longer repeat lengths, consistent with our results. In the other previous study (Ross et al., 2011), the controls might have included some number of presymptomatic patients because the mean age of the controls was lower than that of the PD patients.

In reference to the recent studies concerning the effect of polyQ repeat length on neurodegenerative disease, we screened for a threshold of the normal *ATXN2* polyQ repeat length around a range from 24 to 34 (Charles et al., 2007; Chen et al., 2011; Elden et al., 2010; Gispert et al., 2012; Lee et al., 2011a, 2011b; Ross et al., 2011). The distribution of our patients differed significantly from that of controls only when the cutoff was set to 25. This may be much lower than the threshold for *ATXN2*-related PD adopted by previous studies (Charles et al., 2007), but it is possible that the cutoff for *ATXN2* polyQ repeat length and its influence on PD may vary from population to population, as is the case for ALS, as indicated in a previous study (Lee et al., 2011b). Such variation of the threshold would be consistent with the observation that previous reports of *ATXN2*-associated PD have mainly been from East Asian populations (Charles et al., 2007; Klein et al., 2009; Lu et al., 2004b; Sun et al., 2011; Wang et al., 2009). Additional factors, such as cis- and trans-acting genetic elements, non-allelic genetic modifiers, and stochastic and environmental factors (Charles et al., 2007; Pulst et al., 2005), might have enhanced the toxicity of *ATXN2* intermediate-length polyQ expansion in our population.

We described the details of family members with *ATXN2* intermediate-length expansions (>24 Qs, Fig. 2 and Supplementary Table 2). These patients generally manifested typical PD phenotypes without motor neuron signs, cerebellar ataxia, or saccadic eye movement disorder, as was stated in previous reports (Furtado et al., 2004; Klein et al., 2009). A correlation between the association of AAO and polyQ repeat length was not clearly present or absent in our patients with repeat lengths of *ATXN2* > 24, as previously observed (Furtado et al., 2002, 2004; Payami et al., 2003; Sun et al., 2011). For example, in family A, members of the third generation had earlier AAOs than did their mother. However, there was a gap between the AAOs of AIII-1 and AIII-3, even though their genotypes were the same. In addition, AIII-1 and AIII-3 had 2 allele expansions (35/32 Qs) instead of a single allele expansion, which might have caused their early onsets (Ragothaman et al., 2004). The 35Q alleles may have been inherited "as is" from AII-1, who reportedly had no neurologic disorder, although it is also possible that an expansion occurred upon transmission. Thus, AAOs might be affected by features other than polyQ repeat length, such as genetic and epigenetic factors.

In the present study, we did not find any association between the ADPD phenotype and the repeat lengths of polyQ disease genes other than *ATXN2*. This result implies that the contribution of *ATXN2* to ADPD is because of the specific effects of this gene rather than the presence of the polyQ expansion itself, as reported in a previous study of ALS (Lee et al., 2011a). This result might appear to be inconsistent with recent reports suggesting that the intermediate polyQ expansion of *TBP* is likely to be a risk factor for PD (Kim et al., 2009; Wu et al., 2004; Xu et al., 2010; Yun et al., 2011). However, because those reports did not provide significant evidence, and because all of these studies were performed in East Asian patients, further evidence should be accumulated.

As a supplementary analysis, we also applied a multiple logistic regression including the product terms *ATXN1* × *ATXN2*, *ATXN2* × *ATXN3*, and *ATXN2* × *CACNA1A* to screen for some interactions among these polyQ disease gene combinations, based on previous studies showing the possibility of interaction among these polyQ genes (Al-Ramahi et al., 2007; Jardim et al., 2003; Lessing and Bonini, 2008; Pulst et al., 2005). However, no significant difference was detected between the PD patients and controls (with a threshold p-value of 0.05, Supplementary Table 3).

In conclusion, an intermediate-length polyQ expansion of *ATXN2* is likely to contribute to the pathogenesis of ADPD, either directly causing the PD phenotype or modifying the effects of unknown genes on the PD phenotype. Our results add to the recent finding that intermediate-length polyQ repeat expansions of *ATXN2* may be a contributing factor in multiple neurodegenerative diseases.

Disclosure statement

The authors declare no conflicts of interest.

Acknowledgements

The authors thank all the participants in this study. This work was supported by a Strategic Research Foundation Grant-in-Aid Project for Private Universities; Grants-in-Aid for Scientific Research (to Nobutaka Hattori, 80218510 and to Hiroyuki Tomiyama, 21591098); a Grant-in-Aid for Young Scientists (to Manabu Funayama, 22790829 and to Yuanzhe Li, 23791003); a Grant-in-Aid for Scientific Research on Innovative Areas (to Nobutaka Hattori, 23111003 and to Manabu Funayama, 23129506) from the Japanese Ministry of Education, Culture, Sports, and Science and Technology; Grants-in-Aid from the Research Committee of CNS Degenerative Diseases and Perry Syndrome (to Nobutaka Hattori and Hiroyuki Tomiyama, 22140901); a grant from Health and Labour Sciences Research Grants (to Nobutaka Hattori, 20261501 and 22140501) from the Japanese Ministry of Health, Labour and Welfare, and CREST from the Japan Science and Technology Agency.

Appendix A. Supplementary data

Supplementary data associated with this article can be found, in the online version, at http://dx.doi.org/10.1016/j.neurobiolaging.2014.01.022.

References

Al-Ramahi, I., Perez, A.M., Lim, J., Zhang, M., Sorensen, R., de Haro, M., Branco, J., Pulst, S.M., Zoghbi, H.Y., Botas, J., 2007. dAtaxin-2 mediates expanded ataxin-1-induced neurodegeneration in a Drosophila model of SCA1. PLoS Genet. 3, e234. http://dx.doi.org/10.1371/journal.pgen.0030234.

Bertoni, A., Giuliano, P., Galgani, M., Rotoli, D., Ulianich, L., Adornetto, A., Santillo, M.R., Porcellini, A., Avvedimento, V.E., 2011. Early and late events induced by polyQ-expanded proteins: identification of a common pathogenic property of polyQ-expanded proteins. J. Biol. Chem. 286, 4727–4741. http://dx.doi.org/10.1074/jbc.M110.156521.

Charles, P., Camuzat, A., Benammar, N., Sellal, F., Destee, A., Bonnet, A.M., Lesage, S., Le Ber, I., Stevanin, G., Durr, A., Brice, A., 2007. Are interrupted SCA2 CAG repeat expansions responsible for parkinsonism? Neurology 69, 1970–1975. http://dx.doi.org/10.1212/01.wnl.0000269323.21969.db.

Chen, X., Burgoyne, R.D., 2012. Identification of common genetic modifiers of neurodegenerative diseases from an integrative analysis of diverse genetic screens in model organisms. BMC Genomics 13, 71. http://dx.doi.org/10.1186/1471-2164-13-71.

Chen, Y., Huang, R., Yang, Y., Chen, K., Song, W., Pan, P., Li, J., Shang, H.F., 2011. Ataxin-2 intermediate-length polyglutamine: a possible risk factor for Chinese patients with amyotrophic lateral sclerosis. Neurobiol. Aging 32, 1925.e1–1925.e5. http://dx.doi.org/10.1016/j.neurobiolaging.2011.05.015.

Dubourg, O., Durr, A., Cancel, G., Stevanin, G., Chneiweiss, H., Penet, C., Agid, Y., Brice, A., 1995. Analysis of the SCA1 CAG repeat in a large number of families with dominant ataxia: clinical and molecular correlations. Ann. Neurol. 37, 176–180. http://dx.doi.org/10.1002/ana.410370207.

Elden, A.C., Kim, H.J., Hart, M.P., Chen-Plotkin, A.S., Johnson, B.S., Fang, X., Armakola, M., Geser, F., Greene, R., Lu, M.M., Padmanabhan, A., Clay-Falcone, D., McCluskey, L., Elman, L., Juhr, D., Gruber, P.J., Rub, U., Auburger, G., Trojanowski, J.Q., Lee, V.M., Van Deerlin, V.M., Bonini, N.M., Gitler, A.D., 2010. Ataxin-2 intermediate-length polyglutamine expansions are associated with increased risk for ALS. Nature 466, 1069–1075. http://dx.doi.org/10.1038/nature09320.

Furtado, S., Farrer, M., Tsuboi, Y., Klimek, M.L., de la Fuente-Fernandez, R., Hussey, J., Lockhart, P., Calne, D.B., Suchowersky, O., Stoessl, A.J., Wszolek, Z.K., 2002. SCA-2 presenting as parkinsonism in an Alberta family: clinical, genetic, and PET findings. Neurology 59, 1625–1627.

Furtado, S., Payami, H., Lockhart, P.J., Hanson, M., Nutt, J.G., Singleton, A.A., Singleton, A., Bower, J., Utti, R.J., Bird, T.D., de la Fuente-Fernandez, R., Tsuboi, Y., Klimek, M.L., Suchowersky, O., Hardy, J., Calne, D.B., Wszolek, Z.K., Farrer, M., Gwinn-Hardy, K., Stoessl, A.J., 2004. Profile of families with parkinsonism-predominant spinocerebellar ataxia type 2 (SCA2). Mov. Disord. 19, 622–629. http://dx.doi.org/10.1002/mds.20074.

Gispert, S., Kurz, A., Waibel, S., Bauer, P., Liepelt, I., Geisen, C., Gitler, A.D., Becker, T., Weber, M., Berg, D., Andersen, P.M., Kruger, R., Riess, O., Ludolph, A.C., Auburger, G., 2012. The modulation of amyotrophic lateral sclerosis risk by ataxin-2 intermediate polyglutamine expansions is a specific effect. Neurobiol. Dis. 45, 356–361. http://dx.doi.org/10.1016/j.nbd.2011.08.021.

Gwinn-Hardy, K., Chen, J.Y., Liu, H.C., Liu, T.Y., Boss, M., Seltzer, W., Adam, A., Singleton, A., Koroshetz, W., Waters, C., Hardy, J., Farrer, M., 2000. Spinocerebellar ataxia type 2 with parkinsonism in ethnic Chinese. Neurology 55, 800–805.

Hands, S., Sinadinos, C., Wyttenbach, A., 2008. Polyglutamine gene function and dysfunction in the ageing brain. Biochim. Biophys. Acta 1779, 507–521. http://dx.doi.org/10.1016/j.bbagrm.2008.05.008.

Hughes, A.J., Daniel, S.E., Kilford, L., Lees, A.J., 1992. Accuracy of clinical diagnosis of idiopathic Parkinson's disease: a clinico-pathological study of 100 cases. J. Neurol. Neurosurg. Psychiatry 55, 181–184.

Jardim, L., Silveira, I., Pereira, M.L., do Ceu Moreira, M., Mendonca, P., Sequeiros, J., Giugliani, R., 2003. Searching for modulating effects of SCA2, SCA6 and DRPLA CAG tracts on the Machado-Joseph disease (SCA3) phenotype. Acta Neurol. Scand. 107, 211–214.

Kim, J.M., Lee, J.Y., Kim, H.J., Kim, J.S., Kim, Y.K., Park, S.S., Kim, S.E., Jeon, B.S., 2010. The wide clinical spectrum and nigrostriatal dopaminergic damage in spinocerebellar ataxia type 6. J. Neurol. Neurosurg. Psychiatry 81, 529–532. http://dx.doi.org/10.1136/jnnp.2008.166728.

Kim, J.Y., Kim, S.Y., Kim, J.M., Kim, Y.K., Yoon, K.Y., Lee, B.C., Kim, J.S., Paek, S.H., Park, S.S., Kim, S.E., Jeon, B.S., 2009. Spinocerebellar ataxia type 17 mutation as a causative and susceptibility gene in parkinsonism. Neurology 72, 1385–1389. http://dx.doi.org/10.1212/WNL.0b013e3181a18876.

Klein, C., Schneider, S.A., Lang, A.E., 2009. Hereditary parkinsonism: Parkinson disease look-alikes—an algorithm for clinicians to "PARK" genes and beyond. Mov. Disord. 24, 2042–2058. http://dx.doi.org/10.1002/mds.22675.

Lee, T., Li, Y.R., Chesi, A., Hart, M.P., Ramos, D., Jethava, N., Hosangadi, D., Epstein, J., Hodges, B., Bonini, N.M., Gitler, A.D., 2011a. Evaluating the prevalence of polyglutamine repeat expansions in amyotrophic lateral sclerosis. Neurology 76, 2062–2065. http://dx.doi.org/10.1212/WNL.0b013e31821f4447.

Lee, T., Li, Y.R., Ingre, C., Weber, M., Grehl, T., Gredal, O., de Carvalho, M., Meyer, T., Tysnes, O.B., Auburger, G., Gispert, S., Bonini, N.M., Andersen, P.M., Gitler, A.D., 2011b. Ataxin-2 intermediate-length polyglutamine expansions in European ALS patients. Hum. Mol. Genet. 20, 1697–1700. http://dx.doi.org/10.1093/hmg/ddr045.

Lessing, D., Bonini, N.M., 2008. Polyglutamine genes interact to modulate the severity and progression of neurodegeneration in Drosophila. PLoS Biol. 6, e29. http://dx.doi.org/10.1371/journal.pbio.0060029.

Li, Y., Sekine, T., Funayama, M., Li, L., Yoshino, H., Nishioka, K., Tomiyama, H., Hattori, N., 2013. Clinicogenetic study of GBA mutations in patients with familial Parkinson's disease. Neurobiol. Aging. http://dx.doi.org/10.1016/j.neurobiolaging.2013.09.019.

Lu, C.S., Chang, H.C., Kuo, P.C., Liu, Y.L., Wu, W.S., Weng, Y.H., Yen, T.C., Chou, Y.H., 2004a. The parkinsonian phenotype of spinocerebellar ataxia type 3 in a Taiwanese family. Parkinsonism Relat. Disord. 10, 369–373. http://dx.doi.org/10.1016/j.parkreldis.2004.03.009.

Lu, C.S., Wu Chou, Y.H., Kuo, P.C., Chang, H.C., Weng, Y.H., 2004b. The parkinsonian phenotype of spinocerebellar ataxia type 2. Arch. Neurol. 61, 35–38. http://dx.doi.org/10.1001/archneur.61.1.35.

Mitsui, J., Mizuta, I., Toyoda, A., Ashida, R., Takahashi, Y., Goto, J., Fukuda, Y., Date, H., Iwata, A., Yamamoto, M., Hattori, N., Murata, M., Toda, T., Tsuji, S., 2009. Mutations for Gaucher disease confer high susceptibility to Parkinson disease. Arch. Neurol. 66, 571–576. http://dx.doi.org/10.1001/archneurol.2009.72.

Payami, H., Nutt, J., Gancher, S., Bird, T., McNeal, M.G., Seltzer, W.K., Hussey, J., Lockhart, P., Gwinn-Hardy, K., Singleton, A.A., Singleton, A.B., Hardy, J., Farrer, M., 2003. SCA2 may present as levodopa-responsive parkinsonism. Mov. Disord. 18, 425–429. http://dx.doi.org/10.1002/mds.10375.

Pulst, S.M., Nechiporuk, A., Nechiporuk, T., Gispert, S., Chen, X.N., Lopes-Cendes, I., Pearlman, S., Starkman, S., Orozco-Diaz, G., Lunkes, A., DeJong, P., Rouleau, G.A., Auburger, G., Korenberg, J.R., Figueroa, C., Sahba, S., 1996. Moderate expansion of a normally biallelic trinucleotide repeat in spinocerebellar ataxia type 2. Nat. Genet. 14, 269–276. http://dx.doi.org/10.1038/ng1196-269.

Pulst, S.M., Santos, N., Wang, D., Yang, H., Huynh, D., Velazquez, L., Figueroa, K.P., 2005. Spinocerebellar ataxia type 2: polyQ repeat variation in the CACNA1A calcium channel modifies age of onset. Brain 128 (Pt 10), 2297–2303. http://dx.doi.org/10.1093/brain/awh586.

Ragothaman, M., Sarangmath, N., Chaudhary, S., Khare, V., Mittal, U., Sharma, S., Komatireddy, S., Chakrabarti, S., Mukerji, M., Juyal, R.C., Thelma, B.K., Muthane, U.B., 2004. Complex phenotypes in an Indian family with homozygous SCA2 mutations. Ann. Neurol. 55, 130–133. http://dx.doi.org/10.1002/ana.10815.

Ross, O.A., Rutherford, N.J., Baker, M., Soto-Ortolaza, A.I., Carrasquillo, M.M., DeJesus-Hernandez, M., Adamson, J., Li, M., Volkening, K., Finger, E., Seeley, W.W., Hatanpaa, K.J., Lomen-Hoerth, C., Kertesz, A., Bigio, E.H., Lippa, C., Woodruff, B.K., Knopman, D.S., White 3rd, C.L., Van Gerpen, J.A., Meschia, J.F., Mackenzie, I.R., Boylan, K., Boeve, B.F., Miller, B.L., Strong, M.J., Uitti, R.J., Younkin, S.G., Graff-Radford, N.R., Petersen, R.C., Wszolek, Z.K., Dickson, D.W., Rademakers, R., 2011. Ataxin-2 repeat-length variation and neurodegeneration. Hum. Mol. Genet. 20, 3207–3212. http://dx.doi.org/10.1093/hmg/ddr227.

Sequeiros, J., Seneca, S., Martindale, J., 2010. Consensus and controversies in best practices for molecular genetic testing of spinocerebellar ataxias. Eur. J. Hum. Genet. 18, 1188–1195. http://dx.doi.org/10.1038/ejhg.2010.10.

Subramony, S.H., Hernandez, D., Adam, A., Smith-Jefferson, S., Hussey, J., Gwinn-Hardy, K., Lynch, T., McDaniel, O., Hardy, J., Farrer, M., Singleton, A., 2002. Ethnic differences in the expression of neurodegenerative disease: Machado-Joseph disease in Africans and Caucasians. Mov. Disord. 17, 1068–1071. http://dx.doi.org/10.1002/mds.10241.

Sun, H., Satake, W., Zhang, C., Nagai, Y., Tian, Y., Fu, S., Yu, J., Qian, Y., Chu, J., Toda, T., 2011. Genetic and clinical analysis in a Chinese parkinsonism-predominant spinocerebellar ataxia type 2 family. J. Hum. Genet. 56, 330–334. http://dx.doi.org/10.1038/jhg.2011.14.

Walker, F.O., 2007. Huntington's disease. Lancet 369, 218–228. http://dx.doi.org/10.1016/S0140-6736(07) 60111-1.

Wang, J.L., Xiao, B., Cui, X.X., Guo, J.F., Lei, L.F., Song, X.W., Shen, L., Jiang, H., Yan, X.X., Pan, Q., Long, Z.G., Xia, K., Tang, B.S., 2009. Analysis of SCA2 and SCA3/MJD repeats in Parkinson's disease in mainland China: genetic, clinical, and positron emission tomography findings. Mov. Disord. 24, 2007–2011. http://dx.doi.org/10.1002/mds.22727.

Wu, Y.R., Lin, H.Y., Chen, C.M., Gwinn-Hardy, K., Ro, L.S., Wang, Y.C., Li, S.H., Hwang, J.C., Fang, K., Hsieh-Li, H.M., Li, M.L., Tung, L.C., Su, M.T., Lu, K.T., Lee-Chen, G.J., 2004. Genetic testing in spinocerebellar ataxia in Taiwan: expansions of trinucleotide repeats in SCA8 and SCA17 are associated with typical Parkinson's disease. Clin. Genet. 65, 209–214.

Xu, Q., Jia, D., Wang, J., Guo, J., Jiang, H., Lei, L., Shen, L., Pan, Q., Xia, K., Yan, X., Tang, B., 2010. Genetic analysis of spinocerebellar ataxia type 17 in Parkinson's disease in Mainland China. Parkinsonism Relat. Disord. 16, 700–702. http://dx.doi.org/10.1016/j.parkreldis.2010.08.020.

Yun, J.Y., Lee, W.W., Kim, H.J., Kim, J.S., Kim, J.M., Kim, S.Y., Kim, J.Y., Park, S.S., Kim, Y.K., Kim, S.E., Jeon, B.S., 2011. Relative contribution of SCA2, SCA3 and SCA17 in Korean patients with parkinsonism and ataxia. Parkinsonism Relat. Disord. 17, 338–342. http://dx.doi.org/10.1016/j.parkreldis.2011.01.015.

Parkinsonism and Related Disorders 20 (2014) 659–661

Contents lists available at ScienceDirect

Parkinsonism and Related Disorders

journal homepage: www.elsevier.com/locate/parkreldis

Short communication

EIF4G1 gene mutations are not a common cause of Parkinson's disease in the Japanese population

Kenya Nishioka [a,b], Manabu Funayama [b,c], Carles Vilariño-Güell [d], Kotaro Ogaki [a,b], Yuanzhe Li [b], Ryogen Sasaki [e], Yasumasa Kokubo [e], Shigeki Kuzuhara [f], Jennifer M. Kachergus [a], Stephanie A. Cobb [a], Hirohide Takahashi [g], Yoshikuni Mizuno [b], Matthew J. Farrer [d], Owen A. Ross [a,*], Nobutaka Hattori [b]

[a] Department of Neuroscience, Mayo Clinic, Jacksonville, FL, USA
[b] Department of Neurology, Juntendo University School of Medicine, Tokyo, Japan
[c] Research Institute for Diseases of Old Age, Graduate School of Medicine, Juntendo University, Tokyo, Japan
[d] Department of Medical Genetics, University of British Columbia, Vancouver, Canada
[e] Graduate School of Regional Innovation Studies, Kii ALS/PDC Research Center, Mie University, Tsu, Mie, Japan
[f] Department of Medical Welfare, Faculty of Health Science, Suzuka University of Medical Science, Suzuka, Mie, Japan
[g] Department of Neurology, Tokai University School of Medicine, Kanagawa, Japan

ARTICLE INFO

Article history:
Received 27 December 2013
Received in revised form
25 February 2014
Accepted 1 March 2014

Keywords:
Parkinson's disease
EIF4G1
Mutation
Genetics

ABSTRACT

Pathogenic mutations in the *EIF4G1* gene were recently reported as a cause of autosomal dominant parkinsonism. To assess the frequency of *EIF4G1* mutations in the Japanese population we sequenced the entire gene coding region (31 exons) in 95 patients with an apparent autosomal dominant inherited form of Parkinson's disease. We detected three novel point mutations located in a poly-glutamic acid repeat within exon 10. These variants were screened through 224 Parkinson's disease cases and 374 normal controls from the Japanese population. We detected the poly-glutamic acid deletion in exon 10 in two additional patients with sporadic Parkinson's disease. Although the *EIF4G1* variants identified in the present study were not observed in control subjects, co-segregation analyses and population-based screening data suggest they are not pathogenic. In conclusion, we did not identify novel or previously reported pathogenic mutations (including the p.A502V and p.R1205H mutants) within *EIF4G1* in the Japanese population, thus future studies are warranted to elucidate the role of this gene in Parkinson's disease.

1. Introduction

Parkinson's disease (PD) is one of the most common movement disorders in the elderly. Pathogenic mutations that result in hereditary forms of PD/parkinsonism are reported in a number of genes and have subsequently directed both functional studies and the generation of disease model systems [1,2]. The nomination of each new gene for parkinsonism implicates disease pathways and provides a rationale for targeted therapeutic development [3,4]. Recently, two substitutions in the eukaryotic translation initiation factor 4-gamma 1 protein (*EIF4G1*, MIM#600495); p.R1205H and p.A502V were nominated to cause PD with autosomal dominant inheritance in a number of pedigrees [5]. Furthermore studies in a yeast model revealed the *EIF4G1* ortholog (TIF4632) is a suppressor of α-synuclein toxicity [6].

EIF4G1 is a protein scaffold subunit of the translation initiation complex, EIF4F, which binds the ribosomal 40S. A decrease in the levels of EIF4G1 protein in cells results in a reduction of overall protein synthesis linked to nutrient sensing [7]. Reported pathogenic EIF4G1 substitutions, p.R1205H and p.A502V, were shown to disrupt binding to EIF3E and EIF4E respectively, and result in impaired nutrient sensing and mitochondrial dysfunction [5,7]. Interestingly, over-expression of EIF4G1 protein has been implicated in cell proliferation as observed in some malignant disorders, especially inflammatory breast cancer [8]. This evidence supports a role for *EIF4G1* mutations in cell survival and potentially the neuronal damage observed in PD. Herein, we set out to examine the

* Corresponding author. Department of Neuroscience, Mayo Clinic, 4500 San Pablo Road, Jacksonville, FL 32224, USA. Tel.: +1 904 953 6280; fax: +1 904 953 7370.
E-mail address: ross.owen@mayo.edu (O.A. Ross).

http://dx.doi.org/10.1016/j.parkreldis.2014.03.004
1353-8020/

Table 1
Demographic of patients and control subjects.

Subjects	Ethnicity	No.	Male to female ratio	Mean age at onset (SD)
Autosomal dominant PD	Japanese	95	1:1.32	52.7 (±11.4)
Replication				
Autosomal dominant PD	Japanese	43	1:0.95	41.7 (±14.2)
Sporadic PD	Japanese	181	1:0.91	38.6 (±12.3)
Control subjects	Japanese	374	1:1.49	

PD; Parkinson's disease.
SD; standard deviation.

occurrence and frequency of mutations in the *EIF4G1* gene among PD patients of Japanese origin.

2. Subjects and methods

All individuals were collected at Juntendo University, Tokyo and at Mie University, Mie and were of Japanese ethnicity. Patients were diagnosed with PD based on the modified United Kingdom Parkinson's disease society brain bank criteria. DNA was extracted from peripheral blood by standard protocols. A series of 95 patients with autosomal dominant PD had an average of age at onset of 52.7 years ± 11.4 (SD) and a 1:1.32 male to female ratio were selected (Table 1). Family history was defined as one or more affected relatives within 2 degrees of relationship. All variants were then screened through a population-based patient-control series of 224 patients with PD including 43 probands (age at onset 41.7 ± 14.2 years old and male:female = 1:0.95) with possible autosomal dominant PD, 181 sporadic PD cases (age at onset 38.6 ± 12.3 years old and male:female = 1:0.91) and 374 normal controls (age at examination 57.8 ± 12.6 years old and male:female = 1:1.49). The ethical review boards at the Mayo Clinic, Juntendo University and at Mie University approved the study, and all participants provided informed written consent.

3. Genetic analysis

The 31 coding exons (exon 3–33, NM_198241.2) of *EIF4G1* were sequenced in 95 patients with apparent autosomal dominant PD. Primer pairs for coding regions of *EIF4G1* (exons 3–33) were used and are available upon request [5]. PCR products were purified from unincorporated nucleotides using Agencourt bead technology (Beverly, MA) with Biomek FX automation (Beckman Coulter, Fullerton, CA). Electropherograms were analyzed with SeqScape v2.1.1 using 3730 DNA Analyzer (ABI, Applied Biosystems, Foster City, CA, USA). In addition, real-time PCR was employed to investigate the role of exon dosage and gene copy number variation was analyzed as previously described [5]. We also screened any novel mutations identified and the previously reported mutants (EIF4G1 p.R1205H and p.A502V) in an additional 43 autosomal dominant PD patients, 181 sporadic patients and 374 controls. We performed allelic cloning using a TOPO® TA Cloning® Kit (Life Technologies, Carlsbad, CA, USA) followed by individual clone PCR and sequencing to assess the phase of three exon 10 variants identified in one PD patient.

4. Results

We identified novel *EIF4G1* mutations in one patient with autosomal dominant PD (J-19) among the 95 probands (Supplemental Fig. 1). Patient J-19 had three point mutations; [p.E463G, c.1388AG>GA] and [p.E465A, c.1394A>C] on the same allele, in exon 10 (Fig. 1(a)). However we found the three point mutations in two healthy siblings of patient J-19 (73-year old man and 67-year old woman). In addition, our sequencing analysis identified four novel synonymous variants; p.Q149Q (c.447A>G), p.K1206K (c.3618G>A), p.T1211T (c.3633G>A), and p.Y1488Y (c.4464C>T) which were observed independently each in a single autosomal dominant PD patient (n = 95). No *EIF4G1* gene copy number variations were observed in 95 probands.

Screening an additional 43 patients with autosomal dominant PD and 181 sporadic PD patients, identified two sporadic patient (ID#1558, 1601) with the same three point mutations as patient J-19. Furthermore, one of the two patients (ID#1601) had a known 9 bp deletion (rs111659103) in exon 10 (Fig. 1(b)); these exon 10 variants were not observed in our 374 normal control subjects, but rs111659103 is reported on the Exome Variant Server database with a carrier frequency of over 5%.

5. Discussion

Our comprehensive screening of the coding region of the *EIF4G1* gene in 95 probands from families with apparent autosomal dominant inheritance of PD did not detect any novel pathogenic mutations, nor the p.A502V or p.R1205H variants described in Chartier-Harlin et al. [5]. Several novel variants were identified, including a number of point mutations located in a poly-glutamic acid tract. However the location of the poly-glutamic acid tract

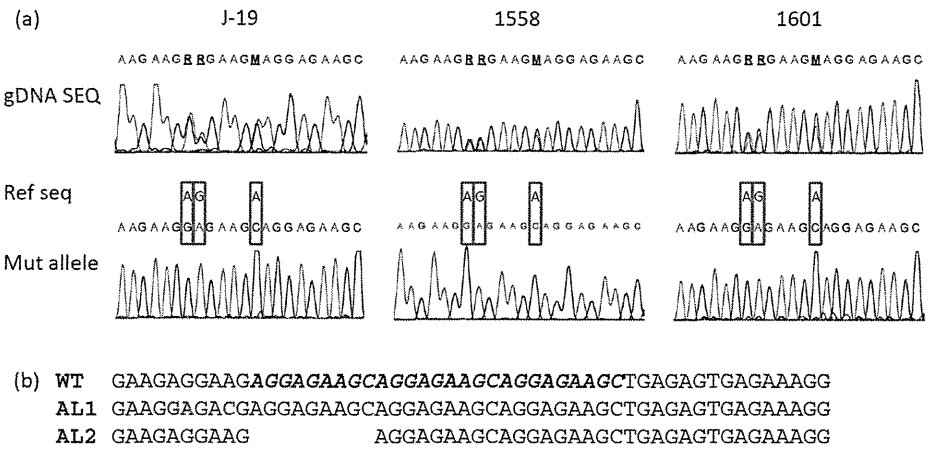

Fig. 1. (a) Genomic sequence of the *EIF4G1* exon 10 from the patients J-19, 1558 and 1601 showing three point mutations; [p.E463G, c.1388AG>GA], and [p.E465A, c.1394A>C], as well as the mutant haplotype from the TOPO TA cloning. The three mutations exist on same allele. (b) Diagrammatic representation of the wild-type sequence around the poly-glutamic acid repeat and highlighting the three point mutations (AL1; red) and 9 bp deletion (AL2; rs111659103) in *EIF4G1* exon 10 from sporadic patient 1601. A three unit perfect repeat (bold in WT allele) precludes determining which unit is rs111659103. (For interpretation of the references to color in this figure legend, the reader is referred to the web version of this article.)

does not appear to be in a region involved in complex formation or RNA-binding, therefore if these variants do have a functional influence the mechanism is yet to be determined. *In silico* analysis using PolyPhen-2 (http://genetics.bwh.harvard.edu/pph2/) predicts the [p.E463G, c.1388AG>GA] and [p.E465A, c.1394A>C] to be both possibly damaging and benign based on HumDiv and HumVar measures respectively. In addition, evidence from disease co-segregation analysis within families, *in silico* prediction and population frequency data from the Exome Variant Server database (rs111659103) does not support variants in the poly-glutamic acid tract as high penetrant pathogenic factors for parkinsonism.

These findings support the initial report describing a relatively low frequency of *EIF4G1* mutations in 4708 individuals with idiopathic PD (7/4708) [5]. Recently, independent studies examining the frequency of *EIF4G1* variation have identified both the p.A502V and p.R1205H variants in non-diseased individuals, thus demonstrating the importance of replication studies to resolve the role of *EIF4G1* variants in PD pathophysiology (Supplemental Table 1). In addition, findings from other *EIF4G1* gene screening studies suggest that mutations are rare in patients across multiple populations and that the pathogenicity of this gene in PD remains to be resolved (Supplemental Table 1). We conclude from our data that *EIF4G1* mutations are not a common cause of PD in patients of Japanese origin.

Given the technological advances in DNA sequencing approaches an ever increasing number of rare variants will be nominated as pathogenic in PD and related neurodegenerative disorders. As observed for *EIF4G1* variants, even large series of patients and controls may not be sufficient to confer definitive pathogenicity. There will need to be large collaborative consortia efforts as recently reported to determine the true nature of rare variants within the context of disease risk and clinical relevance [9,10]. In the absence of overwhelming genetic evidence we may have to rely on a functional readout (e.g. PINK1/PARKIN mutation effects on cellular mitophagy), although reliable disease-specific assays are still to be developed for PD-related genes [11,12]. With the noted caveats in mind further investigations are warranted to confirm the pathogenicity of *EIF4G1* variants in PD and to assess global prevalence and clinical relevance to disease.

Acknowledgment

This work was supported by the Morris K. Udall Center, National Institute of Neurological Disorders and Stroke P50 NS072187 and the Michael J. Fox Foundation for Parkinson's Research. KN was supported by an Eli-Lilly scholarship and Herb Geist gift for Lewy body research.

Appendix A. Supplementary data

Supplementary data related to this article can be found at http://dx.doi.org/10.1016/j.parkreldis.2014.03.004.

References

[1] Sundal C, Fujioka S, Uitti RJ, Wszolek ZK. Autosomal dominant Parkinson's disease. Parkinsonism Relat Disord 2012;18(Suppl. 1):S7–10.
[2] Bonifati V. Autosomal recessive parkinsonism. Parkinsonism Relat Disord 2012;18(Suppl. 1):S4–6.
[3] Valente EM, Arena G, Torosantucci L, Gelmetti V. Molecular pathways in sporadic PD. Parkinsonism Relat Disord 2012;18(Suppl. 1):S71–3.
[4] Puschmann A, Bhidayasiri R, Weiner WJ. Synucleinopathies from bench to bedside. Parkinsonism Relat Disord 2012;18(Suppl. 1):S24–7.
[5] Chartier-Harlin MC, Dachsel JC, Vilarino-Guell C, Lincoln SJ, Lepretre F, Hulihan MM, et al. Translation initiator EIF4G1 mutations in familial Parkinson disease. Am J Hum Genet 2011;89:398–406.
[6] Yeger-Lotem E, Riva L, Su LJ, Gitler AD, Cashikar AG, King OD, et al. Bridging high-throughput genetic and transcriptional data reveals cellular responses to alpha-synuclein toxicity. Nat Genet 2009;41:316–23.
[7] Ramirez-Valle F, Braunstein S, Zavadil J, Formenti SC, Schneider RJ. eIF4GI links nutrient sensing by mTOR to cell proliferation and inhibition of autophagy. J Cell Biol 2008;181:293–307.
[8] Silvera D, Arju R, Darvishian F, Levine PH, Zolfaghari L, Goldberg J, et al. Essential role for eIF4GI overexpression in the pathogenesis of inflammatory breast cancer. Nat Cell Biol 2009;11:903–8.
[9] Lesage S, Brice A. Role of Mendelian genes in "sporadic" Parkinson's disease. Parkinsonism Relat Disord 2012;18(Suppl. 1):S66–70.
[10] Ross OA, Soto-Ortolaza AI, Heckman MG, Aasly JO, Abahuni N, Annesi G, et al. Association of LRRK2 exonic variants with susceptibility to Parkinson's disease: a case-control study. Lancet Neurol 2011;10:898–908.
[11] Kawajiri S, Saiki S, Sato S, Sato F, Hatano T, Eguchi H, et al. PINK1 is recruited to mitochondria with parkin and associates with LC3 in mitophagy. FEBS Lett 2010;584:1073–9.
[12] Geisler S, Holmstrom KM, Skujat D, Fiesel FC, Rothfuss OC, Kahle PJ, et al. PINK1/Parkin-mediated mitophagy is dependent on VDAC1 and p62/SQSTM1. Nat Cell Biol 2010;12:119–31.

BASIC RESEARCH PAPER

Autophagy 10:4, 631–641; April 2014; © 2014 Landes Bioscience

PARK2/Parkin-mediated mitochondrial clearance contributes to proteasome activation during slow-twitch muscle atrophy via NFE2L1 nuclear translocation

Norihiko Furuya,[1,†,‡,*] Shin-Ichi Ikeda,[2] Shigeto Sato,[3] Sanae Soma,[1] Junji Ezaki,[1] Juan Alejandro Oliva Trejo,[1] Mitsue Takeda-Ezaki,[1] Tsutomu Fujimura,[4] Eri Arikawa-Hirasawa,[3,5] Norihiro Tada,[5] Masaaki Komatsu,[6] Keiji Tanaka,[7] Eiki Kominami,[1] Nobutaka Hattori,[3] and Takashi Ueno[1,§,*]

[1]Department of Biochemistry; Juntendo University School of Medicine; Bunkyo-ku, Tokyo Japan; [2]Sportology Center; Juntendo University Graduate School of Medicine; Bunkyo-ku, Tokyo Japan; [3]Department of Neurology; Juntendo University School of Medicine; Bunkyo-ku, Tokyo Japan; [4]Laboratory of Proteomics and Biomolecular Science; Research Support Center; Juntendo University Graduate School of Medicine; Bunkyo-ku, Tokyo Japan; [5]Research Institute for Diseases of Old Age; Juntendo University Graduate School of Medicine; Bunkyo-ku, Tokyo Japan; [6]Protein Metabolism Project; Tokyo Metropolitan Institute of Medical Science; Setagaya-ku, Tokyo Japan; [7]Laboratory of Protein Metabolism; Tokyo Metropolitan Institute of Medical Science; Setagaya-ku, Tokyo Japan

Current affiliation: [†]Department of Research and Therapeutics for Movement Disorders; Juntendo University Graduate School of Medicine; Bunkyo-ku, Tokyo Japan; [‡]Department of Neurology; Juntendo University School of Medicine; Bunkyo-ku, Tokyo Japan; [§]Laboratory of Proteomics and Biomolecular Science; Research Support Center; Juntendo University Graduate School of Medicine; Bunkyo-ku, Tokyo Japan

Keywords: PARK2-mediated mitophagy, skeletal muscle atrophy, proteasome, NFE2L1, slow-twitch muscle, autophagy, mitochondria, knockout mouse

Abbreviations: ARE, antioxidant response element; CCCP, carbonyl cyanide m-chlorophenylhydrazone; NAC, N-acetyl-cysteine; NFE2L1, nuclear factor erythroid-derived 2-related factor 1; NFE2L2, nuclear factor erythroid-derived 2-related factor 2; ROS, reactive oxygen species; tBHQ, tert-butyl hydroquinone

Skeletal muscle atrophy is thought to result from hyperactivation of intracellular protein degradation pathways, including autophagy and the ubiquitin–proteasome system. However, the precise contributions of these pathways to muscle atrophy are unclear. Here, we show that an autophagy deficiency in denervated slow-twitch soleus muscles delayed skeletal muscle atrophy, reduced mitochondrial activity, and induced oxidative stress and accumulation of PARK2/Parkin, which participates in mitochondrial quality control (PARK2-mediated mitophagy), in mitochondria. Soleus muscles from denervated *P*ark2 knockout mice also showed resistance to denervation, reduced mitochondrial activities, and increased oxidative stress. In both autophagy-deficient and *Park2*-deficient soleus muscles, denervation caused the accumulation of polyubiquitinated proteins. Denervation induced proteasomal activation via NFE2L1 nuclear translocation in control mice, whereas it had little effect in autophagy-deficient and *Park2*-deficient mice. These results suggest that PARK2-mediated mitophagy plays an essential role in the activation of proteasomes during denervation atrophy in slow-twitch muscles.

Introduction

Skeletal muscles occupy up to 55% of total body mass in mammals, and generate motile forces and heat. They are a major site for carbohydrate and fatty acid metabolism and are categorized into 2 types exhibiting distinct contractile and metabolic properties: slow-twitch, oxidative fatigue-resistant muscles and fast-twitch, glycolytic fatigue-susceptible muscles. The slow-twitch muscle fibers typically display a 2- to 3-fold higher mitochondrial density and substantially lower capacity for nonoxidative ATP synthesis compared with the fast-twitch muscle fibers.

Maintenance of muscle mass depends on a balance between protein synthesis and degradation. Innervation of skeletal muscle fibers by motor neurons is essential for maintenance of muscle size, structure, and function. Numerous disorders, including amyotrophic lateral sclerosis, Guillain-Barre syndrome, polio, and polyneuropathy, disrupt the nerve supply to muscle, causing

*Correspondence to: Norihiko Furuya; Email: nohuruya@juntendo.ac.jp; Takashi Ueno; Email: upfield@juntendo.ac.jp
Submitted: 08/20/2013; Revised: 01/06/2014; Accepted: 01/09/2014
http://dx.doi.org/10.4161/auto.27785

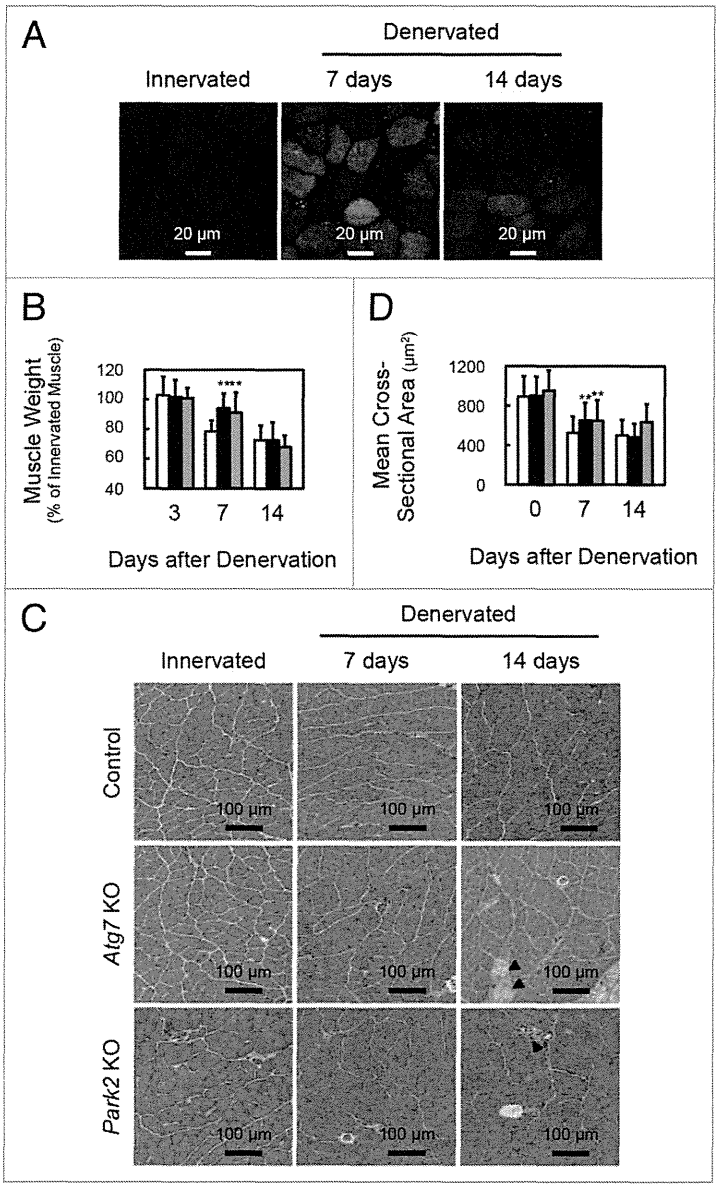

Figure 1. Delay of denervation atrophy in autophagy-deficient and PARK2-deficient soleus muscle. (**A**) Representative images of soleus muscles from GFP-LC3 transgenic mice at 0 (innervated), 7 and 14 d after denervation. Scale bar, 20 μm. (**B**) Time course of weight loss in the soleus muscles of denervated mice. For the denervation procedure, the left sciatic nerves of control mice (open bar: day 3, n = 9; day 7, n = 28; day 14, n = 19), *Atg7* KO mice (closed bar: day 3, n = 12; day 7, n = 30; day 14, n = 14) or *Park2* KO mice (gray bar: day 3, n = 3; day 7, n = 13; day 14, n = 7) were cut in the mid-thigh region, leading to denervation of the lower limb muscles. Denervated muscle weight data are shown as the percentage of the weight of the contralateral innervated muscle from the right limb. Data are shown as the means ± s.d. $^{**}P < 0.01$ vs control mice at the same time. (**C**) Histological analysis of control, *Atg7* KO and *Park2* KO soleus muscles. Cryosections were stained with hematoxylin and eosin. Arrowheads, dead myofibers. Scale Bars: 100 μm. (**D**) Quantification of the cross-sectional areas of myofibers. Values are the means ± s.d. vs control mice at the same time, $^{**}P < 0.01$.

loss of muscle mass strength and endurance (referred to as neurogenic atrophy).[1,2] Other pathological states and systemic disorders, including cancer, diabetes, fasting, sepsis, and disuse, also cause muscle atrophy. The resulting loss of muscle mass in these conditions involves an activation of intracellular protein degradation and a decrease in protein synthesis. The ubiquitin-proteasome system (UPS) and autophagy are the 2 major pathways leading to intracellular degradation, and, when upregulated by the activation of FOXO transcription factors, both systems can contribute to skeletal muscle atrophy.[3-6]

The UPS is responsible for biologically important cellular processes including cell cycle progression, DNA repair, signaling cascades, cell death, immunity, developmental programs, and protein quality control by catalyzing selective degradation of regulatory proteins and damaged proteins.[7,8] Macroautophagy (hereafter referred to as autophagy) is a membrane dynamic process in which cytoplasmic components including macromolecules and organelles are sequestered into double-membrane structures called autophagosomes and delivered to lysosomes for degradation.[9,10] Autophagy participates not only in supplying amino acids under nutrient-poor environments, but also in the clearance of misfolded or aggregated proteins, damaged organelles, and pathogens. Currently, the differences between the contributions of the UPS and autophagy to the process of muscle atrophy are not clear.

Results

Autophagy is required for the early steps of denervation atrophy in soleus muscle

To ascertain whether autophagy is activated in atrophying muscles, we subjected GFP-LC3 transgenic mice[11] to denervation of the sciatic nerve, a model of skeletal muscle atrophy (**Fig. 1A**; **Fig. S1A**). Many GFP-LC3 puncta were observed in both slow-twitch soleus muscles and fast-twitch plantaris muscles of mice at 7 and 14 d after denervation. In the initial stage (within 48 h) of denervation atrophy, autophagy is suppressed by the proteasome-dependent MTORC1 activation.[12] However, these results show that autophagy is activated in atrophying hind-limb muscles. As previously reported, autophagy deficiency in skeletal muscle causes more muscle loss owing to denervation than occurs in the control situation with normal autophagy, and autophagy is required to maintain muscle mass.[4] However the contribution of autophagy to the process of muscle atrophy is not clear. We generated mice with a skeletal muscle-specific *Atg7* (an essential gene for autophagy) knockout under the control of the tamoxifen-inducible human skeletal actin (HSA) promoter ($Atg7^{Flox/Flox}$: HSA-Cre-ER^{T2}, hereinafter referred to as *Atg7* KO mice), and subjected them to denervation. The plantaris muscles, a fast-twitch glycolytic skeletal muscle, from both *Atg7* KO and control ($Atg7^{Flox/Flox}$) mice, were atrophied to almost the

same extent by denervation (**Fig. S1B**). In contrast, the soleus muscle, a slow-twitch oxidative skeletal muscle, from *Atg7* KO mice, showed resistance to denervation at 7 d after denervation (**Fig. 1B–D**; **Fig. S2A**). However, the soleus muscles from *Atg7* KO mice and control mice exhibited comparable muscle mass and myofiber size at 14 d after denervation. Notably, dead myofibers were frequently observed in the *Atg7* KO soleus muscles at 14 d (**Fig. 1C**). The enhanced cell death at 14 d most likely contributes to the shrinking of the soleus muscle of *Atg7* KO mice. The phenotypes of soleus muscles of *Atg7* KO mice at 14 d after denervation are coincident with the previous study.[4] However, the phenotypes at a period earlier than 14 d after denervation were not investigated in that study. Thus, our finding seemed to reflect a more direct effect of autophagy-deficiency on muscle atrophy. These results indicated that autophagy contributes to the early stage of denervation atrophy and that autophagy deficiency delays atrophy in soleus muscle. In contrast, autophagy in fast-twitch muscles seems not to play an important role in the early stage of denervation atrophy, in spite of its activation by denervation in GFP-LC mice.

Denervated soleus muscle from *Atg7* KO mice shows mitochondrial dysfunction

To elucidate the precise phenotypes of the soleus muscles of denervated *Atg7* KO mice at 7 d after denervation, histological analyses were performed (**Fig. 2A**). The ratio of type I to type II muscle fibers in both innervated and denervated soleus muscles was almost the same in control and *Atg7* KO mice. Meanwhile, denervated soleus muscles from *Atg7* KO mice exhibited reduced staining for succinate dehydrogenase (SDH; complex II) and cytochrome *c* oxidase (Cox; complex IV) compared with denervated soleus muscles from control mice (**Fig. 2A and B**), indicating that the respiratory chain activities of denervated soleus muscles of *Atg7* KO mice were significantly decreased. The reduction of respiratory chain activities was not observed in denervated plantaris muscles from *Atg7* KO mice (**Fig. S1D**). As frequently reported for other autophagy-deficient mice, electron microscopy analysis revealed that abnormally swollen mitochondria were observed in the soleus muscles of denervated *Atg7* KO mice (**Fig. 2C**),[13-16] whereas, most of the mitochondria were morphologically normal in the soleus muscles of denervated *Atg7* KO mice. As was the case in GFP-LC3 mice, denervation induced formation of autophagic vacuoles (AVs) in the soleus muscles of control mice, whereas AVs were rarely observed in denervated soleus muscles of *Atg7* KO mice (**Fig. 2C**). These results indicated that autophagy deficiency leads to abnormal accumulation of mitochondria in the denervated soleus muscles. However, the expression levels of marker proteins for the outer membrane (e.g., TOMM20/Tom20), the intermembrane space (e.g., CYCS/cytochrome *c*), the inner membrane (e.g., OPA1), and the matrix (e.g., PDHA1/pyruvate dehydrogenase α1;) of mitochondria, and PPARGC1A/PGC1α, a master regulator of mitochondrial biogenesis, in denervated soleus muscles from *Atg7* KO mice, were comparable to those in the denervated muscles of control mice (**Fig. 2D**; **Fig. S2B**). The expression levels of DNM1L/Drp1 and FIS1/Fis1, which promote the fragmentation of mitochondria (Romanello et al., 2010), were not influenced by denervation. Mitochondrial DNA (mtDNA) copy numbers in denervated *Atg7* KO soleus muscles were not different from those in denervated control soleus muscles (**Fig. 2E**; **Fig. S2C**). Taken together, these results indicate that the decreased respiratory chain activities of denervated *Atg7* KO soleus muscle can be attributed to a qualitative reduction in mitochondrial function, but not to a decreased quantity of mitochondria. It is important to clarify the reason for the reduced mitochondrial function in denervated *Atg7* KO soleus muscles. Generally, oxidative stress is inseparably associated with dysregulation or disruption of mitochondrial functions, because mitochondria are both generators and targets of reactive oxygen species (ROS).[17] To ascertain whether ROS accumulate in denervated *Atg7* KO soleus muscles, we performed immunostaining with an antibody against 8-hydroxydeoxyguanosine (8-OHdG), a marker of ROS (**Fig. S3**). The denervated *Atg7* KO soleus muscles accumulated much more 8-OHdG than did the denervated control or the innervated *Atg7* KO soleus muscles. Moreover, the accumulation of carbonylated proteins was greater in denervated *Atg* KO soleus muscles than in denervated control or innervated *Atg7* KO muscles (**Fig. 2D**). These results suggest that denervated *Atg7* KO soleus muscles accumulate damaged mitochondria, which have reduced respiratory chain activities and produce abundant ROS.

PARK2 is required for denervation atrophy of soleus muscle

The E3 ubiquitin ligase PARK2/Parkin is commonly mutated in autosomal recessive juvenile parkinsonism.[18] Upon mitochondrial damage or uncoupling, PARK2 localizes to mitochondria and mediates the ubiquitination of mitochondrial outer membrane proteins and the autophagic elimination of damaged mitochondria (mitophagy), thereby participating in mitochondrial quality control.[19,20] Denervation induced PARK2 expression in hind-limb muscles (**Fig. 3A and B**; **Fig. S1C**) and the level of PARK2 expression induced by denervation was much higher in soleus muscles than in plantaris muscles. In addition to PARK2 expression, MFN1, a PARK2 substrate, accumulated in denervated soleus muscles from *Atg7* KO mice. In contrast, another E3 ubiquitin ligase, MUL1, which is involved in mitophagy during skeletal muscle atrophy,[21] was not induced by denervation in soleus and plantaris muscles. Subcellular fractionation experiments revealed that the mitochondrial fraction of the soleus muscles of denervated *Atg7* KO mice showed an accumulation of PARK2 (**Fig. 3C**). Immunofluorescence microscopy of cryosections of soleus muscles revealed colocalization of fragmented mitochondria and PARK2 in perinuclear regions of muscle fibers in denervated *Atg7* KO mice (**Fig. 3D**). These results indicate that damaged mitochondria associated with PARK2 are not eliminated and accumulate in the soleus muscles of denervated *Atg7* KO mice because of the deficiency of autophagy, and suggest that the contribution of PARK2 to mitochondrial clearance in denervated slow-twitch soleus muscles is much larger than it is in fast-twitch muscles, probably owing to the abundance of mitochondria. To confirm whether the PARK2-mediated mitophagy is involved in the denervation atrophy in the soleus muscles, we denervated *Park2*-deficient (*Park2* KO) mice.[22] Intriguingly, as was the

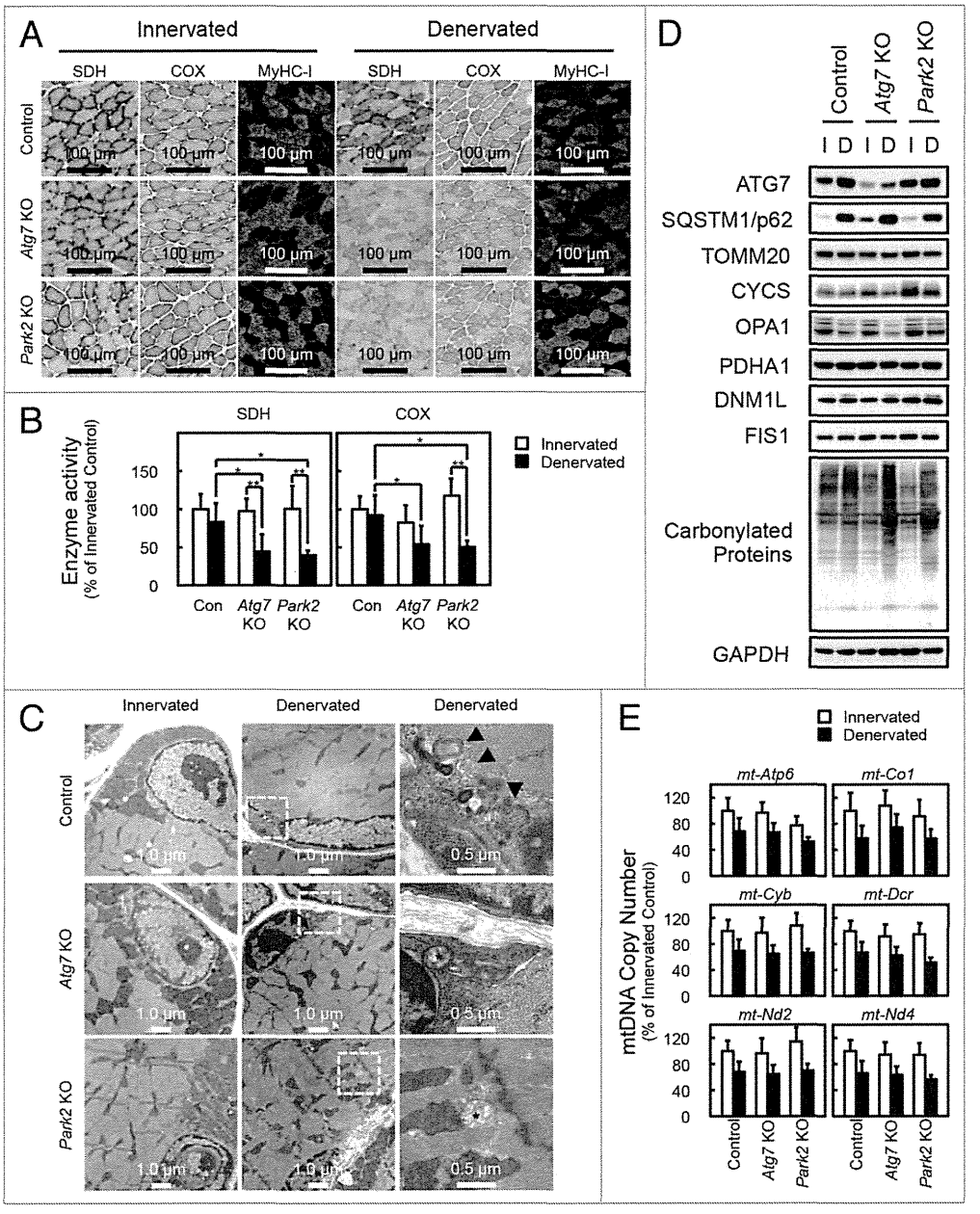

Figure 2. Denervation mediates mitochondrial damage in *Atg7* KO and *Park2* KO soleus muscles. (**A**) Histological analysis and immunofluorescence analysis of soleus muscles from control, *Atg7* KO and *Park2* KO mice 7 d after denervation. Histochemical detection of succinate dehydrogenase (SDH) and cytochrome *c* oxidase (COX) activities in cryosections of soleus muscles and immunofluorescence images of denervated soleus muscles stained with anti-myosin heavy chain I (MyHC-I, green) and anti-DMD (red) antibodies. Nuclei were visualized with Hoechst 33342 (blue). Scale bars, 100 μm. (**B**) Quantitative analysis of SDH and COX activities of soleus muscles shown in a. $^{*}P < 0.05$, $^{**}P < 0.01$. (**C**) Electron micrographs of control, *Atg7* KO, and *Park2* KO soleus muscles at 7 d after denervation. Innervated limb and denervated limb are shown. The boxed regions in the middle panels are shown in the next panels on the right. Arrowhead, autophagic vacuole or phagophore membrane; asterisk, abnormal mitochondrion. (**D**) Western blot analysis of soleus muscles from mice at 7 d after denervation. Whole tissue lysates of the denervated (D) and the contralateral innervated (I) soleus muscles were immunoblotted with antibodies against the indicated proteins. The data shown are representative of at least 3 separate experiments. (**E**) Changes in mitochondrial DNA (mtDNA) copy numbers caused by denervation of soleus muscles. mtDNA copy numbers were quantified by real-time PCR to detect mtDNA-coded genes. Data are shown as the percentage of the values (mean ± s.d.) obtained from innervated soleus muscles from control mice.

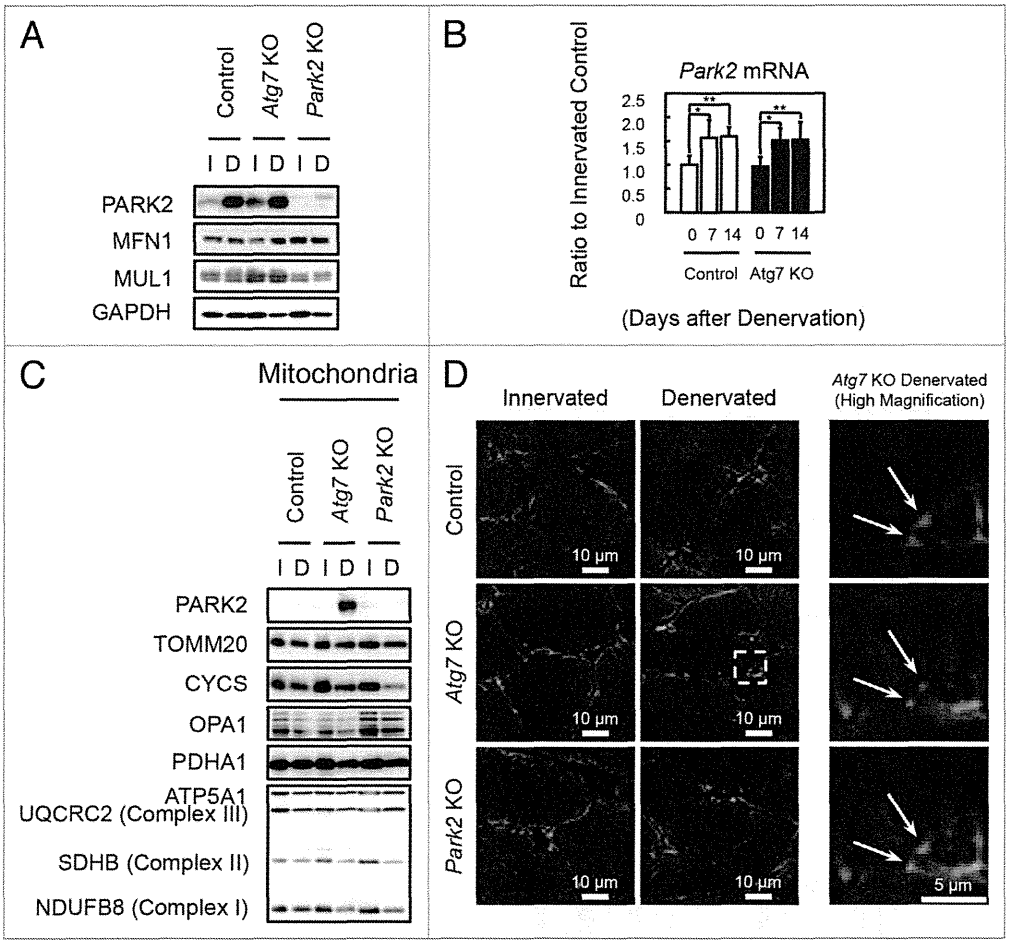

Figure 3. PARK2 accumulates in damaged mitochondria in denervated soleus muscles from *Atg7* KO mice. (**A**) Western blot analysis of soleus muscles from mice at 7 d after denervation with antibodies against the indicated proteins. (**B**) Quantification of *Park2* mRNA levels by real-time PCR in soleus muscles. Values are shown as ratios to the mRNA levels in innervated soleus muscles from control mice. The data are means ± s.d. vs. innervated (day 0) muscle from each genotype, $^{**}P < 0.01$. (**C**) Western blot analysis of mitochondrial fractions from soleus muscles. Mitochondrial fractions prepared from denervated (D) and innervated (I) soleus muscles of the indicated genotypes at 7 d after denervation and immunoblotted with anti-PARK2 antibody and antibodies against mitochondrial markers. (**D**) Immunofluorescent micrographs of denervated (7 d) or innervated soleus muscles of the indicated genotypes stained with anti-PARK2 (red) or anti-TOMM20 (mitochondrial marker, green) antibodies and Hoechst 33342 (nucleus, blue). Colocalization of fragmented mitochondria with PARK2 was observed in denervated *Atg7* KO soleus muscles. Boxed areas in denervated soleus muscles are shown in the next panels on the right.

case with *Atg7* KO mice, the soleus muscles from *Park2* KO mice retained muscle mass 7 d after denervation (**Fig. 1**). In addition, a reduction in their mitochondrial respiratory chain complex activities and accumulation of ROS were observed 7 d after denervation (**Fig. 2A–C**; **Fig. S3**). Together, these results indicate that the PARK2-mediated mitochondrial quality control pathway is required for the early stage of denervation atrophy of soleus muscles. A *Drosophila parkin*-null mutant shows obvious phenotypes including locomotive defects, muscle degeneration, and mitochondrial swelling in the flight muscles.[23-25] Indirect flight muscles, a group of specialized muscles with high mitochondria content, require a high oxygen supply to sustain their respiratory activity for a constant vibration. In mammals, slow-twitch muscles also contain more mitochondria than fast-twitch muscles. Thus, it is possible that mitochondria-rich muscles are more susceptible to the lack of PARK2-mediated mitophagy than other tissues.

PARK2-mediated mitophagy is required for proteasomal activation in denervated soleus muscle

To evaluate the mechanism underlying the delay of soleus muscle atrophy in denervated *Atg7* KO and *Park2* KO mice, we initially assumed the participation of the GDF8/myostatin signaling pathway and anti-apoptotic BCL2 family members in those phenotypes. However, denervation of wild-type, *Atg7* KO, and *Park2* KO mice resulted in very similar expression patterns for myostatin, myostatin receptor, and BCL2 family members in soleus muscles, indicating that none of these was related to the mechanism of atrophy (**Fig. S2B and S2D**). Finally, we noticed the accumulation of polyubiquitinated proteins in the soleus muscles of denervated *Atg7* KO and denervated *Park2* KO mice (**Fig. 4A**).

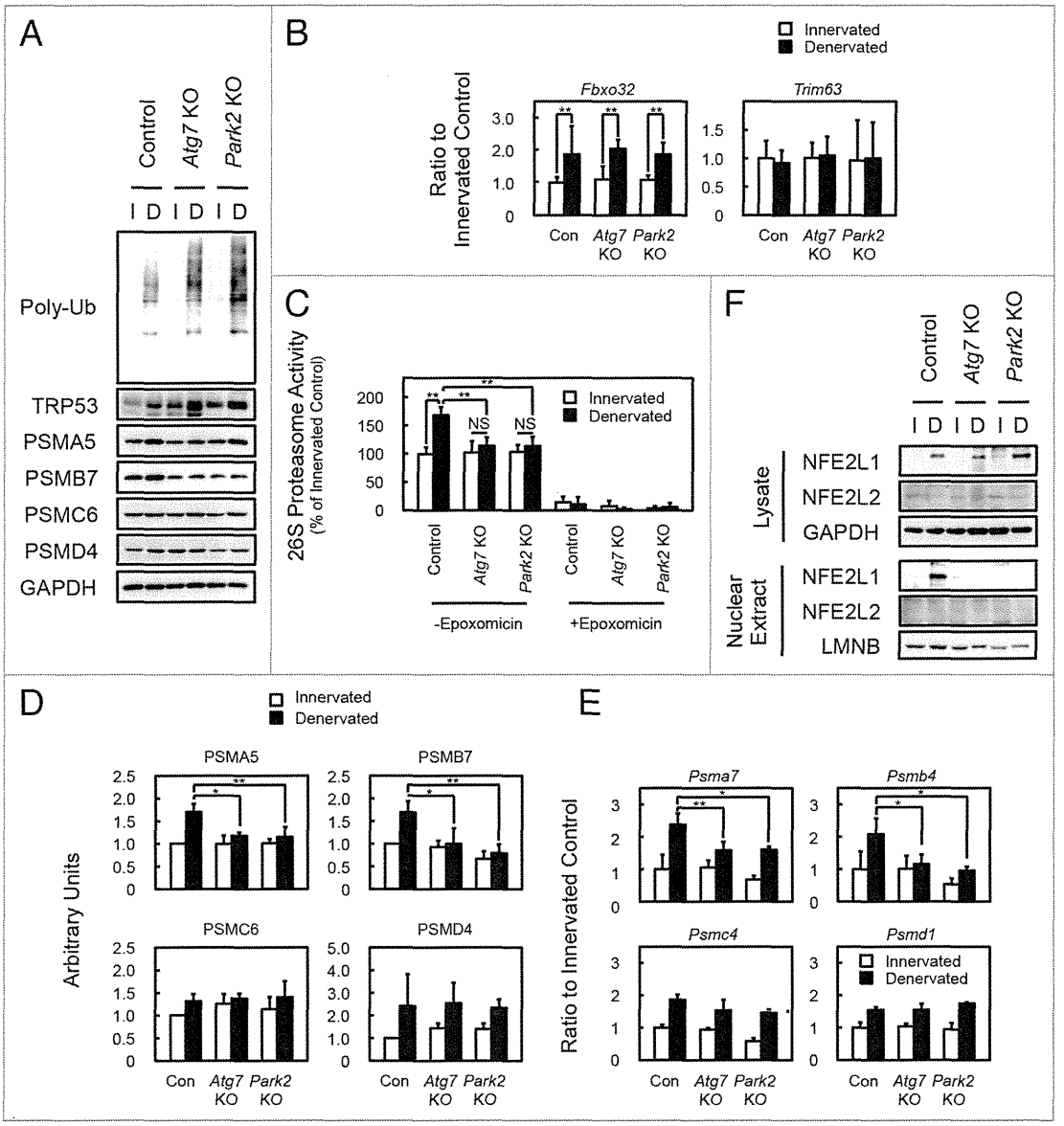

Figure 4. PARK2-mediated mitophagy is required for the activation of 26S proteasomes in denervated soleus muscle. (**A**) Western blot analysis of soleus muscles. Whole-tissue lysates of soleus muscles were immunoblotted with antibodies against the indicated proteins. The data shown are representative of at least 3 separate experiments. (**B**) Quantification of the mRNA levels for atrophy-related E3 ubiquitin ligases (*Fbxo32* and *Trim63*) in soleus muscles by real-time PCR. Data are shown as the ratios (mean ± s.d.) to the mRNA levels obtained from innervated soleus muscles from control mice. $^{**}P < 0.01$. (**C**) Peptide hydrolysis activity of 26S proteasomes. Soleus muscle homogenates from *Atg7* KO, *Park2* KO, and control mice were used to assay the chymotryptic activity of proteasomes using Suc-LLVY-AMC as a substrate in the absence or presence of 20 μM epoxomicin. Data are shown as the percentage of the activity (mean ± s.d.) obtained from innervated soleus muscles from control mice. $^{**}P < 0.01$, NS; not significant. (**D**) Quantitative densitometry of immunoblotting data for the proteasome subunits shown in a. $^{*}P < 0.05$, $^{**}P < 0.01$. (**E**) Quantification of the mRNA levels of proteasome subunits in soleus muscles by real-time PCR. Data are shown as the ratios (mean ± s.d.) to the mRNA levels obtained from innervated soleus muscles from control mice. $^{*}P < 0.05$, $^{**}P < 0.01$ vs denervated muscle from control mice. (**F**) Nuclear levels of NFE2L1 in soleus muscles. Nuclear extracts prepared from denervated and innervated soleus muscles and total tissue lysates were immunoblotted with anti-NFE2L1, anti- NFE2L2, anti-LMNB (as a loading control for nuclear extracts), and GAPDH (as a loading control for tissue lysates) antibodies. The data shown are representative of at least 3 separate experiments.

In addition, the soleus muscles of denervated *Atg7* KO and *Park2* KO mice accumulated more polyubiquitinated proteins than did the plantaris muscles of those animals (**Fig. S4A**). It has been reported that the accumulation of polyubiquitinated proteins is a hallmark of autophagy-deficient tissues,[13-16] whereas a similar accumulation has not been reported in *Park2*-deficient animals. It is also known that the accumulation of unfolded proteins or protein aggregates interferes with proteasome-mediated protein degradation.[26,27] Therefore, we suspected that the deficiency of PARK2-mediated mitophagy attenuates the activity of the

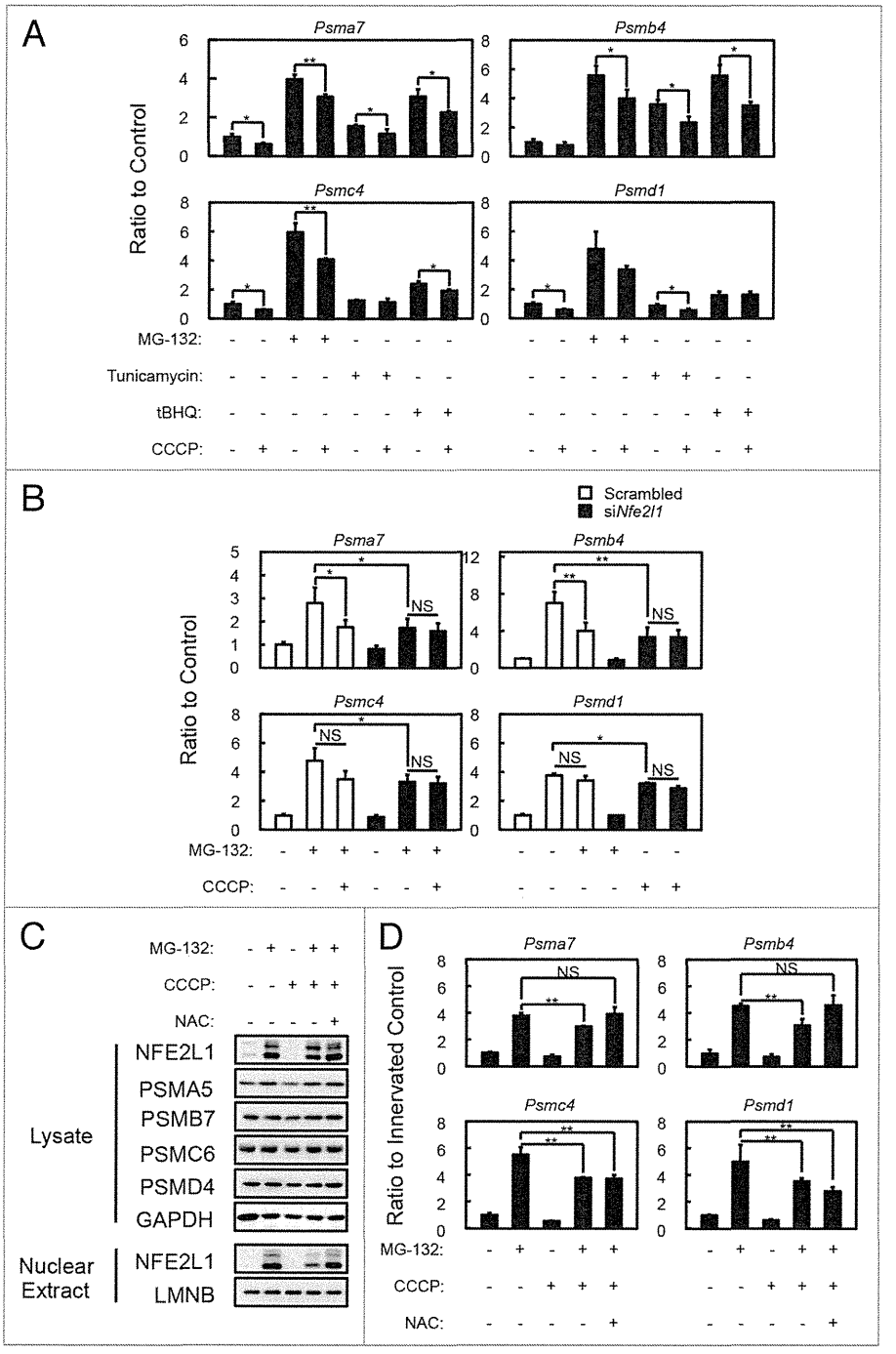

Figure 5. Effects of mitochondrial depolarization on proteasome subunit expression and NFE2L1 nuclear translocation in C2C12 cells. (**A**) Quantification of the mRNA levels of proteasome subunits in C2C12 cells incubated with 10 μM MG-132, 1 μg/ml tunicamycin and 50 μM tBHQ in the presence and absence of 10 μM CCCP for 24 h by real-time PCR. Data are shown as the ratios (mean ± s.d.) to the mRNA levels in the vehicle-treated control cells. $^{*}P < 0.05$, $^{**}P < 0.01$ (Student *t* test). (**B**) Quantification of the mRNA levels of proteasome subunits in si*Nfe2l1* treated C2C12 cells by real-time PCR. C2C12 cells were transfected with si*Nfe2l1* or scrambled siRNA, then incubated with 10 μM MG-132 in the presence and absence of 10 μM CCCP for 24 h. $^{*}P < 0.05$, $^{**}P < 0.01$, NS; not significant. (**C**) Western blot analysis of the cell lysates and nuclear extracts of C2C12 cells. Cell lysates and nuclear extracts of C2C12 cells incubated with 10 μM CCCP and/or 10 μM MG-132 in the presence or absence of 10 mM NAC for 24 h were assayed by western blotting using antibodies against the indicated proteins. The data shown are representative of at least 3 separate experiments. (**D**) Quantitative densitometry of immunoblotting data for the proteasome subunits shown in b. $^{**}P < 0.01$, NS; not significant.

UPS pathway and results in the delay of soleus muscle atrophy in both *Atg7* KO and *Park2* KO mice. Because muscle-specific E3 ubiquitin ligases are known to promote protein degradation during skeletal muscle atrophy,[28,29] we examined the expression levels of *Fbxo32/Mafbx/atrogin-1* and *Trim63/Murf1* using real-time quantitative PCR (**Fig. 4B**). However, the expression levels of *Fbxo32* and *Trim63* in denervated soleus muscles were comparable in all of the genotypes examined. Next, we measured 26S proteasomal activities in tissue extracts from denervated and innervated soleus muscles. In control mice, denervation induced 26S proteasome activities in extracts from soleus muscles. In contrast, denervation did not induce proteasomal activation in extracts from the soleus muscles of *Atg7* KO and *Park2* KO mice (**Fig. 4C**). In addition to proteasomal activities in vitro, we found that denervation increased the levels of the endogenous proteasome substrate TRP53/p53 in the soleus muscles of *Atg7* KO and *Park2* KO mice compared with those in controls (**Fig. 4A**). In the plantaris muscles of all genotypes examined, denervation did not induce the accumulation of TRP53 as in the soleus muscles of *Atg7* KO and *Park2* KO mice (**Fig. S4A**). These results suggest that, owing to a lack of proteasome activation after denervation in the soleus muscles of *Atg7* KO and *Park2* KO mice, more TRP53 accumulated, whereas proteasome activation in the soleus muscles of denervated control mice can result in lower levels of TRP53. To ascertain whether the difference in the amount of proteasome activation caused by denervation in control and KO soleus muscles is due to an increase in the number of proteasomes, we examined protein and mRNA levels